LA-2743

LOS ALAMOS SCIENTIFIC LABORATORY
OF THE UNIVERSITY OF CALIFORNIA o LOS ALAMOS NEW MEXICO

LIFETIME OF NEUTRONS IN REFLECTORS

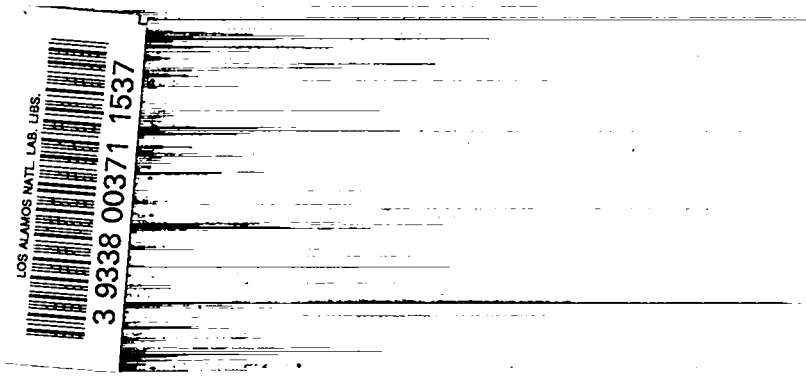

Printed in USA. Price $ 1.75. Available from the

Office of Technical Services
U. S. Department of Commerce
Washington 25, D. C.

LA-2743
PHYSICS
TID-4500 (18th Ed.)

LOS ALAMOS SCIENTIFIC LABORATORY
OF THE UNIVERSITY OF CALIFORNIA LOS ALAMOS NEW MEXICO

REPORT WRITTEN: March 1946
REPORT REVISED: September 1962
REVISION DISTRIBUTED: November 15, 1962

LIFETIME OF NEUTRONS IN REFLECTORS

Work done by:

M. Battat
W. Bright
W. Hane
C. Janney
T. Jorgensen
K. Kupferberg
J. Manley
M. Sands

Report written by:

Kenneth M. Kupferberg

Contract W-7405-ENG. 36 with the U. S. Atomic Energy Commission

ABSTRACT

The mean lifetime of neutrons from a D-D source is measured in U, WC, and BeO reflectors by introducing a short burst of neutrons into the center and observing the subsequent time distribution. The percentage of U^{235} fissions delayed is determined for each of these reflectors, and conclusions are drawn concerning the relative effectiveness of the three materials.

TABLE OF CONTENTS

I. INTRODUCTION

The dynamic characteristics of a fast reactor depend upon the time behavior of neutrons returned to the core by a surrounding reflector. The influence on transient response is of particular interest for application to accident analysis. Neutron lifetime in several reflector materials (U, WC, and BeO) was measured because of limitations in the cross-section data required for computation of such quantities.

The time distribution of the reflected neutrons is investigated by introducing a short burst of neutrons into the center of the reflector and measuring the growth and decay of this short pulse of neutrons with suitable fission detectors and a fast time analyzer. The mean lifetime of the neutrons in the system is obtained from the decay curve after the neutron source is turned off. The measurement of the growth and decay curve, using a fission detector and the fast time analyzer, makes it possible to obtain an estimate of the percentage of fissions which are delayed, the resolving time of the apparatus used in this experiment

being of the order of 10^{-7} sec.

A program of time measurements with U^{235}, U^{238}, and Np^{237} fission chambers has been carried out using a number of reflector materials. The reflectors investigated were U, WC, and BeO.

II. EXPERIMENTAL ARRANGEMENT

A. The D-D Neutron Source.

The neutrons used for the time distribution experiments were obtained from the D-D reaction with 200-kv deuteron ions impinging on a thick heavy-ice (D_2O) target. The 200-kv deuterons were obtained with a linear accelerator, the accelerating voltage being supplied by a Cockcroft-Walton quadrupler. The beam of deuterons emerging from the linear accelerator is magnetically analyzed so that the atomic beam is spatially separated from the molecular beam. The atomic deuteron beam is then collimated by two molybdenum diaphragms with 3/16" diameter apertures. The well-collimated beam strikes the heavy-ice target which is on the face of a cold Cu tube out at 45^{o} to the incident beam. The target was cooled with a liquid oxygen refluxing system. The neutron yield was monitored by counting the protons from the alternate D-D reaction.

The source of D-D neutrons is located at the center of

the spherical cavity within the approximately spherical reflectors. The energy of the neutrons from the modulated D-D source varies from a maximum of 3.1 Mev at 0^{o} to the incident deuteron beam, to a minimum of 2.1 Mev at 180^{o} to the deuteron beam. This energy spectrum covers only a small part of the energy spectrum of fission neutrons from U^{235} or Pu^{239}. Figure 1 shows the general arrangement of the target, and the beam, proton monitor, and cooling tubes. The position of the U reflector with respect to the target assembly also is indicated. For the WC and BeO reflectors, the target was also centrally located, but the dimensions are not the same as those shown in Fig. 1 (see section II G for details).

B. Modulation of the Deuteron Ion Beam.

A short burst of D-D neutrons is obtained by electrically deflecting the deuteron ion beam away from the heavy-ice target for all but a selected short interval of time. A pair of deflecting plates 60 cm long separated by 2.5 cm, is located in the grounded portion of the accelerator tube. A tungsten stop with a rectangular aperture, 1" x 1/4", is located 4" above the deflection plates. The deflected beam keeps this stop at a high enough temperature to prevent the formation on the tungsten of a deuteron gas target which

could yield an undesirable production of neutrons. A D. C. voltage is applied to one of the deflection plates for alignment of the ion beam. The other deflection plate is connected to the modulation circuit (see block diagram, Fig. 2), which applies a potential of approximately 200 volts and at periodic intervals abruptly removes this potential for a chosen interval of time, thus permitting the beam to strike the heavy-ice target and produce a short burst of neutrons. The rectangular voltage pulse generated by the modulator circuit has a rise time of approximately 0.05 μsec, and its duration could be varied from 0.5 to 4.0 μsec in 0.5-μsec steps. The circuit is triggered by pulses from a master oscillator whose frequency can be continuously varied from 50 to 150 kc. The repetition rate of the modulator voltage pulses is so selected as to allow sufficient time for one burst of neutrons to decay in the reflector before another burst is introduced.

This method of modulation of the ion beam presents much less difficulty than modulation of the beam at the ion source which is at high potential (200 kv). However, a disadvantage is the steady but small background of neutrons, caused by two factors: (a) the entire ion beam is not completely deflected onto the tungsten stop above the deflection plates, and therefore can form stray deuterium

targets on the brass walls and defining apertures of the beam tube (4' long), and (b) those deuteron ions which are not in the central part of the focused beam may manage to strike the heavy-ice target even when the beam is deflected. This background can be eliminated by using a larger deflecting potential, but it was not feasible to build a new modulator circuit at the time of the experiment. The steady background was always less than 1% of the peak of the neutron burst and was adequately overcome by experimentally determining its intensity and removing it from the data.

C. Pulse-Time Distribution Equipment.

The pulse-time analyzer, used to measure the time distribution of the burst of neutrons introduced into the reflector, is an electronic circuit which creates a series of eleven rectangular voltage pulses or gates, each of approximately 0.45-μsec duration, which are successively applied to eleven coincidence tubes. The amplified fission pulses from the U^{235} or U^{238} fission chamber are applied to all eleven coincidence tubes. The first gate makes the first coincidence tube conducting for the time interval 0 to 0.45 μsec; therefore, the first coincidence circuit records only those fission pulses occurring in this

time interval. The second gate makes the second coincidence tube conducting for the time interval 0.45 to 0.90 μsec; therefore, the second coincidence circuit records only those fission pulses occurring in this time interval; and so on for the eleven gates. Each coincidence circuit has a counting circuit and mechanical recorder. There exist, therefore, eleven time intervals (commonly referred to as channels) of approximately equal duration, covering a 5-μsec time interval, which make it possible to simultaneously record the entire time distribution of the short burst of neutrons if the growth and decay of this burst of neutrons in the reflector takes place in less than 5 μsec.

The resolution of the pulse-time analyzer is determined by the time during which each channel records the fission pulses. Ideally there would be a large number of channels each of short duration compared with the duration of the burst of neutrons in the reflector, so that the growth and decay could be accurately determined. For this experiment the duration of the modulator pulse was set at 1.0 μsec. Therefore, the pulse of neutrons spread over only two or three channels of the pulse-time analyzer, making it difficult to determine the shape of the neutron burst. To overcome this difficulty, a method of experimental interpolation was devised. The pulse-time analyzer

is triggered by a pulse from the master oscillator, which is synchronized with the pulse triggering the beam modulator circuit. Delaying the pulse that triggers the beam-pulse modulator by a time equal to one-half of one channel width of the pulse-time analyzer makes it possible to obtain eleven points on the pulse-time distribution curve which are intermediate to the eleven points obtained with the undelayed triggering of the beam-pulse modulator.

D. Schematic Arrangement of Apparatus.

Figure 2 is a block diagram of the various circuits involved in the time measurements. The purpose of those circuits which have not yet been discussed is explained as follows:

(1) Master oscillator pulse No. 1 goes through variable delay line No. 1 and triggers the beam-pulse modulator circuit, thereby introducing a short burst of neutrons into the center of the reflector.

(2) Master oscillator pulse No. 2 goes through variable delay line No. 2 and triggers the pulse-time analyzer, beginning the sequence of eleven channels. Delay lines No. 1 and No. 2 are adjusted so that the first channel of the pulse-time analyzer opens at the same instant that the ion beam deflection is counteracted by the modulator circuit.

The desired interpolation points for the pulse-time distribution curve are obtained by adjusting delay line No. 1 so that pulse No. 1 triggers the beam-pulse modulator circuit by a time interval equal to half the channel width after the pulse-time analyzer is triggered.

(3) Master oscillator pulse No. 3 triggers the sweep of the synchroscope 0.2 μsec before the ion beam is undeflected. The target beam current trace on the synchroscope is obtained by applying to the vertical plates of the synchroscope the amplified voltage drop across an 11-megohm resistor between the target and ground (target current circuit, Fig. 2). The scope trace of the target current was an excellent indication of whether the ion beam was properly focused. The trace was thin and well defined when the beam was in good focus. Defocusing the beam by varying the focus voltage caused the trace to become broad and indistinct. During the interval in which the data were accumulated, the scope trace of the target current was continuously monitored to insure a well-defined pulse of neutrons at all times.

(4) After the burst of neutrons has been injected into the center of the reflector, the neutrons which are wandering about in the system are detected by U^{238} and U^{235} (or Np^{237}) fission detectors located at the inner

surface of the reflector (Fig. 1). The fission pulses from each detector are amplified by a fast pre-amplifier and amplifier (LASL Model 500) and fed through separate discriminators which are set to eliminate the background and alpha pulses. The U^{235} fission pulses are fed through adjustable delay line No. 3 so that all these pulses are delayed by a time interval larger than the duration of the beam pulse.

(5) The total number of U^{235} and U^{238} fission pulses is recorded by individual scaling circuits.

(6) The group of U^{238} pulses is fed to one grid of a mixer tube, and the group of U^{235} pulses, which are separated in time from the U^{238} pulses, is fed to the second grid. The U^{238} and U^{235} pulses (which are separated in time) are sharpened by a blocking oscillator circuit. The sharpened pulses have a rise time of less than 0.01 μsec. Mixing the two groups of pulses and keeping the groups separated in time makes only one pulse-time analyzer circuit necessary.

(7) The sharpened U^{235} and U^{238} pulses are applied to all eleven coincidence tubes of the pulse-time analyzer circuit. The pulse-time analyzer records the U^{238} pulse-time distribution in the first three or four channels and the U^{235} pulse-time distribution in the remaining channels.

The repetition rate of the above sequence of events is controlled by the frequency of the master oscillator. The frequency is chosen so that there will be no overlap of successive cycles; that is, one burst of neutrons will have decayed in the system before another burst is injected.

E. Calibration of the Pulse-Time Analyzer and Delay Lines.

To determine the mean life of the neutrons in the reflector from the time distribution of fission pulses recorded by the pulse-time analyzer, it is essential to obtain an accurate calibration of the channel widths, the time interval during which pulses are recorded by each channel. Two independent methods were used for the calibration of the channel widths: (a) the random-count method, and (b) the variable delay line pulser method.

The random-count method involves feeding random pulses into the pulse-time analyzer. The channel width is calculable if the counting rate of each channel, the total counting rate, and the frequency of triggering of the pulse-time analyzer are measured. The counting rate for each channel is given by the expression:

$$N_r = N_t \cdot t_r \cdot f \qquad (1)$$

where

N_r = the counting rate of the r^{th} channel

N_t = the total counting rate

t_r = the width of the r^{th} channel

f = the frequency of triggering of the pulse-time analyzer

The source of random pulses was the neutrons emitted from a 200-mg Ra-Be source and detected by a U^{235} fission detector. To obtain a large random-pulse counting rate, the Ra-Be source and the detector were placed in a large block of paraffin.

The only objection to the random-count method is that it does not give an accurate time scale because there is a finite time overlap or separation of neighboring channels. This is because the rectangular voltage pulses or gates which determine the channel widths do not have an infinitesimal rise time and cut-off time. The pulse-time analyzer was adjusted so that there was a finite overlap of adjacent channels. This is preferable to having gaps between channels. To directly measure the absolute channel widths and the overlap of adjacent channels, a calibrator circuit was constructed. The calibrator is essentially a pulser which feeds pulses through a variable and tapped delay line. Pulse No. 2 from the master oscillator triggers the calibrator so that the pulses produced by the calibrator are synchronized with the triggering of the

pulse-time analyzer, but the repetition rate of the pulses is lowered so that the mechanical recorders for each channel will not jam. It is possible to shift the pulses in time continuously through the time interval of all eleven channels by adjusting the variable and tapped delay line. The beginning, end, and overlap of each channel is then easily observable. The pulse from the calibrator has a rise time of the order of 0.01 μsec which enables the channel widths to be determined to within ±0.02 μsec providing the variable and tapped delay lines of the calibrator are determined to an accuracy of ±0.01 μsec. The average channel width measured was 0.45 μsec, and the overlap of neighboring channels was 0.04 μsec. The channel widths measured by both methods checked to within the experimental accuracy of ±0.02 μsec.

The calibration of the variable and tapped delay line for this calibrator was obtained as follows:

(1) The time standard was a Sickles circular-sweep radar range finder which has a 100-kc crystal controlling the sweep (one circular sweep equals 10 μsec).

(2) This standard was used to calibrate a radar sweep-speed calibrator. The sweep-speed calibrator was adjusted so that it produced a sine wave of 1 Mc frequency (10 cycles on the circular sweep).

(3) The sweep-speed calibrator was used in turn to calibrate the sweep of a radar synchroscope. The fastest sweep of this scope was 0.18 μsec/in.

(4) The synchroscope was in turn used to calibrate the variable and tapped delay line by determining the time shift of the pulse on the scope screen after the pulse has been fed through the delay line.

Delay lines No. 1, No. 2, and No. 3 (Fig. 2) were also calibrated by feeding pulse No. 1, 2, or 3 from the master oscillator through the delay lines and observing the time shift of the pulse on the synchroscope screen.

F. Neutron Detectors.

Spiral fission chambers of the type designed by W. C. Bright (LA-420) were used as neutron detectors. The spiral foils of these detectors were coated with fissionable material, U^{235}, U^{238}, or Np^{237}. The U^{238} fission chamber detects those neutrons having an energy greater than 1.1 Mev, the fission threshold. The Np^{237} fission chamber detects those neutrons having an energy greater than 0.4 Mev, the fission threshold. The U^{235} fission detector covered with a thin cadmium cup (0.025" thick, density 3.6 gm/cc) detects neutrons having an energy greater than 0.22 ev.

The spiral fission chambers have been made in different sizes. The largest cylindrical chamber has outside dimensions of 1" diameter and 1-1/16" length, and the smallest, outside dimensions of 3/8" diameter and 7/16" length (Figs. 3, 6, 7, LA-420). The U^{238} and U^{235} fission chambers used to measure the neutron time distributions were of the largest size. The Np^{237} and U^{238} fission chambers used to obtain the time distribution measurements indicated in Figs. 3 and 4 were of the smallest size.

The rise time of the fission pulses from these detectors, measured with a fast sweep scope, was less than 0.1 μsec (measurement limited by the rise time of the fast amplifier, approximately 0.05 to 0.1 μsec).

G. Reflectors.

The U reflector was in the form of a hollow sphere of outside radius 9-1/2" and inside radius 3-17/32". The WC reflector was built of surface-ground blocks to form roughly a pseudo-sphere of 14-7/8" diameter with a cubical cavity 6-3/4" on a side. The BeO reflector was built of blocks to form a pseudo-sphere of outside radius 9-1/2" having a spherical cavity of radius 3-17/32".

III. ANALYSIS OF DATA AND RESULTS

A. Measurements with Bare Source.

The time distribution of the neutrons emitted from the modulated D-D source was investigated with U^{235}, U^{238}, and Np^{237} fission detectors (no reflector surrounding the target). Two sets of measurements were made with the U^{235} and U^{238} detectors of the largest size, and one set with U^{238} and Np^{237} detectors of the smallest size (see section II F). The distance from the center of the target to the front end of the fission chamber (end nearest target) was 3-17/32" for the large chambers and 1-1/2" for the small chambers. The U^{235} and Np^{237} detectors were at 0^{o} to the incident deuteron beam, and the U^{238} detector was at 90^{o} to the incident beam. The finite rise time of the voltage pulse (0.05×10^{-6} sec) applied to the deflection plates, and the finite diameter of the ion beam make it impossible to obtain a pulse of neutrons which is rectangular (rise time small compared with duration of pulse).

At time t, the counting rate of the fission detector is proportional to the neutron flux through the detector and to the fission cross section of the detector nuclei.

$$f(t) = n(t) \cdot v \cdot \sigma^{f}(v) \cdot A \qquad (2)$$

where

$f(t)$ = number of detected fissions per second at time t

$n(t)$ = neutron density at the position of the detector

v = velocity of the neutrons

A = effective number of detector nuclei (U^{235}, U^{238}, or Np^{237})

$\sigma^f(v)$ = fission cross section of the detector nuclei for neutrons of velocity v

A channel of the pulse-time analyzer counts the number of fission pulses, F(t), occurring at time t in a time interval, Δt, equal to the width of a channel.

$$F(t) = f(t) \cdot \Delta t \tag{3}$$

The pulse-time distribution curves are plots of the number of fissions recorded in each channel versus the time. (Time t is chosen as the center of each channel.) The calibration of the time scale was discussed in section II E.

Since F(t) for the bare source is proportional to the number of neutrons per second emitted from the source at time t, the pulse-time distribution curve, F(t) vs t, is a picture of the time distribution of neutrons emitted from the modulated D-D source. Figures 3, 5, and 6 represent three sets of bare source measurements, taken at regularly spaced intervals during the course of the experiment. For all three sets of bare source measurements, the U^{235} (or

Np^{237}) fission pulses were delayed with respect to the U^{238} fission pulses by a time interval larger than the duration of the modulated neutron source. This made it possible to separate the two sets of data and to determine the shape of the source function with two different fission detectors under the same experimental conditions, using only one pulse-time analyzer. The time distribution obtained with the pulse-time analyzer is only a representative picture of the burst of neutrons if the width of the channels is small compared with the duration of the neutron burst. If the neutron burst occurred in one channel of the pulse-time analyzer, it would be impossible to tell whether or not the burst of neutrons was rectangular. The duration of the beam pulse chosen in this experiment was approximately four times larger than the duration of one channel; therefore, using the experimental interpolation technique described in section II C, it was possible to obtain 8 points for the time-distribution curve, adequate for obtaining a picture of the neutron burst. For Figs. 3 and 5, the interpolation method was used. The interpolation technique was not used for Fig. 6, yet it was possible to draw a smooth curve through the experimental points by knowing the shape of the curves from Figs. 3 and 5. For all three bare-source measurements, the U^{238} data were normalized to the U^{235}

(or Np^{237}) data by multiplying the U^{238} data by the ratio of the U^{235} to U^{238} (or Np^{237} to U^{238}) integral counts as recorded by the scalers (Fig. 2).

The curve that could be fitted to the experimental points for each set of data (U^{235}, U^{238}, or Np^{237}) is of the form

$$F(t) = F\left(\frac{T}{2}\right) \sin^4\left(\frac{\pi t}{T}\right), \qquad 0 \leq t \leq T \qquad (4)$$

where

T = duration of the neutron burst (sec)

F(T/2) = maximum of the bare-source function F(t) at time t = T/2

The value of T for which F(t) best fits the experimental data is T = 1.6 μsec, which corresponds to a pulse of half width (width at half height) of 0.58 μsec.

The ordinate used in all the pulse-time distribution curves is the number of counts recorded by each channel for 1000 clicks of the proton monitor (scale of 64). The 64,000 proton counts from the alternate D-D reaction monitored the neutron yield. The ordinates of each of the curves cannot be compared because the fission-pulse discriminator biases, determining minimum pulse height of the recorded pulses from the fission detectors, may have varied from one reflector experiment to the next. The bias curve

of the fission detectors did not have a plateau, therefore any drift or change in the discriminator settings caused a change in the counting rate. The discriminator biases were set well above the background level.

B. Neutron Mean-Lifetime Measurements.

When the bare source is surrounded by a reflector, the neutron flux through the fission detector is increased by those neutrons which are elastically and inelastically scattered by the surrounding material. The number of fissions vs time curve is not necessarily of the form given by Eq. (4), as in the bare-source measurements, but depends on whether the neutrons are reflected almost immediately (time interval short compared with a resolving time of the apparatus, (0.1 μsec), or whether they wander about in the reflector for a finite (measurable) time before they are removed by radiative capture or leakage out of the system. In general, for an infinite reflector (no leakage), when the source of neutrons is turned off, the neutrons which are still wandering about are absorbed by radiative capture, the probability of radiative capture per second being

$$P_r = N\sigma_r v = \frac{1}{\tau_r} \qquad (5)$$

where

N = number of capturing nuclei per unit volume

v = velocity of the neutrons

σ_r = radiative capture cross section of the reflector nuclei for neutrons of velocity v

τ_r = mean lifetime of the neutrons in the reflector due to radiative capture

For a finite reflector, an estimate of the leakage out of the system can be obtained by using the one-velocity diffusion theory. The probability of leakage of neutrons per second out of a sphere of radius R is

$$P_\ell = \frac{\pi^2 D}{R^2} = \frac{1}{\tau_\ell} \tag{6}$$

$$D = \text{diffusion constant} = \frac{\lambda_{tr} v}{3} = \frac{v}{3N\sigma_{tr}} \tag{7}$$

where

λ_{tr} = transport mean free path for neutrons of velocity v

σ_{tr} = transport cross section for neutrons of velocity v

v = velocity of the neutrons

N = number of scattering nuclei per unit volume

τ_ℓ = mean lifetime of the neutrons in the reflector due to leakage

The diffusion theory is valid only if the probability of scattering of the neutrons is much larger than the

probability of capture.

If $1/\tau_a$ is the probability of leakage and capture of neutrons per sec, then

$$\frac{1}{\tau_a} = \frac{1}{\tau_r} + \frac{1}{\tau_\ell} \tag{8}$$

where τ_a is the mean lifetime of the neutrons due to capture and leakage.

Examination of all the U^{238} fission-pulse time distribution curves for the various reflectors (Figs. 4, 7-12) indicates no essential difference from the shape of the bare-source curve. Since the fission threshold of the U^{238} detector nuclei is 1.1 Mev, the inelastic scattering cross section of the D-D neutrons to energies below 1.1 Mev can be considered as a capture cross section as far as the U^{238} detector is concerned. The mean lifetime due to capture is estimated using Eq. (5), in which σ_r is replaced by the sum of the inelastic scattering and radiative capture cross sections. Taking the average energy of the D-D neutrons as 2.5 Mev and using the value of σ_{in} (inelastic) = 2 barns for U and W (σ_{in} taken intermediate to σ_{in} for 3 Mev neutrons which are inelastically scattered to energies lower than 1.3 Mev and 0.75 Mev; LA-105, Table V), the estimated value of τ_r for U and W is of the order of 5×10^{-9} sec. The mean lifetime due to leakage of neutrons

out of BeO, W, and U reflectors can be estimated using Eq. (6). Using the values of the transport cross sections of 1.5 Mev neutrons in U, W, and BeO (Table IV LA-105), the mean lifetime due to leakage from these reflectors is found to be of the order of 10^{-8} sec. For BeO, τ_{ℓ} is of the order of 5×10^{-8} sec for 0.4-Mev neutrons (Np^{237} fission threshold). Therefore the U^{238} detector time measurements in U, WC, and BeO and the Np^{237} detector time measurements in BeO should indicate no delay greater than 10^{-7} sec. The resolving time of the time-measuring equipment is of the order of 10^{-7} sec; therefore, there should be no measurable delay for the above mentioned cases ($\tau = 10^{-7}$ sec corresponds to $\sigma_{in} = 0.1$ barn). This agrees with all the experimental data obtained using U^{238} and Np^{237} detectors (see Figs. 4, 7-12). The U^{238} time distribution curves for the reflectors investigated can be used as a representative picture of the neutron burst for comparison with the U^{235} time distribution curves.

The U^{235} fission detector, which is sensitive in the entire energy range of interest (0.22 ev to > 3 Mev) was used for the time measurements to determine whether or not the neutrons of energy less than 1.1 Mev (U^{238} fission threshold) have an observable decay time (greater than 0.1 μsec). As was pointed out, there are two processes for the

removal of neutrons, radiative capture and leakage. The radiative capture cross section of neutrons for the heavy elements such as U and W can, for a first order approximation, be considered as having a 1/v dependence above 1 kev. Therefore, the probability for capture can be considered approximately constant throughout the energy interval 1 kev to 1 Mev. The probability of leakage per second out of a sphere (as given by Eq. (6)) increases with increasing velocity v (and σ_{tr} decreases for increasing v); hence, the leakage at high energies is more effective for the removal of neutrons than is the radiative capture process. Figures 13 and 14 are graphs indicating $1/\tau_{\ell}$, $1/\tau_{r}$, and $1/\tau_{a}$ as a function of the energy of the neutrons for spheres of U and WC. The probability of capture per second for U was calculated using the values of the radiative capture cross section given in LA-179, Fig. 3. The probability of capture per second for WC was assumed constant and was calculated at 200 kev using the value σ_{r} = 0.12 barn (Table I, LA-140 (CLASSIFIED)). The probability of leakage per second for WC and U reflectors was calculated using Eq. (6), and it was assumed that the systems with spherical cavities could be considered as solid spheres, so that a first order approximation of the leakage could be easily obtained. The transport cross sections for U were obtained from LA-140

(CLASSIFIED) Fig. 19. The transport cross section for WC was obtained using the values for W given in LA-140, Fig. 19, and the values for C given in LA-256.

If the mean lifetime (τ_a) of the neutrons, which are either captured by the reflector material or leak out, is determined, it is possible to make an estimate of the average energy of the neutrons in the system from the curves of $1/\tau_a$ in Figs. 13 and 14. Examination of Figs. 8-12 indicates that after the source of neutrons is turned off, the U^{235} fissions detected decrease exponentially with time. This exponential decrease can be represented by the familiar decay equation

$$\frac{dF(t)}{dt} = -\frac{F(t)}{\tau_a} \tag{9}$$

where $-1/\tau_a$ is the slope of the ln F(t) vs t curve (Figs. 15-20). F(t) is proportional to the neutron density n(t) (Eq. (2) and (3)). Therefore, for neutrons of average velocity $\bar{v}$,

$$\frac{1}{F(t)}\frac{dF(t)}{dt} = \frac{1}{n(t)}\frac{dn(t)}{dt} \tag{10}$$

If the spectrum of neutrons in the reflector extends over a large range of velocities, and if it is assumed that the material is a 1/v absorber and the probability of leakage is small compared with the probability of capture, it can be shown that Eq. (10) is valid and does not depend on

the spectrum of the neutrons or the energy sensitivity of the fission detector. Consider the spectrum of neutrons as composed of m velocity groups v_1, v_2, ..., v_m, then Eq. (2) can be written as

$$\sum_{i=1}^{m} F_i = \sum_{i=1}^{m} n_i \cdot v_i \cdot \sigma_i^f A \tag{11}$$

Differentiating Eq. (11) and assuming $dv_i/dt = o$ gives

$$\frac{1}{\sum_{i=1}^{m} F_i} \frac{d\left(\sum_{i}^{m} F_i\right)}{dt} = \frac{1}{\sum_{i=1}^{m} F_i} \left[\sum_{i=1}^{m} \left(F_i \cdot \frac{1}{n_i} \frac{dn_i}{dt} \right) \right] \tag{12}$$

If there is only radiative capture in the material and negligible leakage,

$$\frac{1}{n_i} \frac{dn_i}{dt} = - \frac{1}{(\tau_{r_i})} = -N(\sigma_{r_i}) v_i \tag{13}$$

Equation (13) is the familiar exponential decay equation. For a 1/v absorber, $(\sigma_{r_i}) v_i$ is constant for all values of i, and Eq. (12) reduces to

$$\frac{1}{\sum_{i=1}^{m} F_i} \frac{d\left(\sum_{i}^{m} F_i\right)}{dt} = \frac{1}{n_i} \frac{dn_i}{dt} = \text{constant} \tag{14}$$

which is equivalent to Eq. (10) and verifies the statement

made above.

When there is appreciable leakage out of the reflector as compared with radiative capture, $(1/n_i)\,dn_i/dt$ is no longer constant but increases with increasing energy of the neutrons ($1/\tau_a$, Figs. 13 and 14). In this case, after the source of neutrons is turned off, the τ_a observed is a complicated function of the neutron flux for each of the energy groups of the neutron spectrum, and is also a function of the energy dependence of the fission cross section of the detector nuclei and of the scattering and capture cross sections of the reflector nuclei. Therefore, the values of τ_a obtained from the U^{235} fission-pulse-time curve are the representative values of the mean lifetime of the neutrons in the reflector, only if the velocities of the neutrons are in a narrow energy band, or if the material is a 1/v absorber for neutrons and leakage is small compared with radiative capture.

Table 1 contains the values of τ_a obtained from Figs. 15-20. For the U reflector there was no measurable delay after the neutron source was turned off (see Fig. 7); therefore, one can estimate from the calculated curve of $1/\tau_a$ vs energy (Fig. 13), that the average energy of the neutrons in the U reflector is greater than 50 kev if $\tau_a < 10^{-7}$ sec. The value of $\tau_a = 0.3 \pm 0.1$ μsec for the WC

TABLE 1

Neutron Lifetimes and Multiplications of Various Reflectors

Reflector	U^{238} Detector Angle (°)	U^{238} Detector Distance (in.)	U^{235} Detector Angle (°)	U^{235} Detector Distance (in.)	U^{235} Detector Cup	Neutron mean lifetime $\tau_a \times 10^{-6}$ sec	Percentage of U^{235} fissions delayed	Steady state reflector multiplication (LA-304) $M_{st}(U^{238})$	Steady state reflector multiplication (LA-304) $M_{st}(U^{235})$	Effective reflector multiplication $M_{eff}(U^{238})$	Effective reflector multiplication $M_{eff}(U^{235})$
U	45	3-17/32	0	3-17/32	Cd	<0.1	negligible	1.50	5.4	1.50	5.4
WC	90	3-3/16	0	3-3/16	Cd	0.3±0.1	13	1.29	4.71	1.29	4.10
BeO(B)	90	3-17/32	0	3-17/32	Cd	4.9±1	70	1.59	16.6	1.59	4.98
						4.4±1.5	70				
BeO(C)	0	3-17/32	90	3-17/32	Cd	3.8±1	71				
BeO(D)	0	1-1/2	90	1-1/2	B	1.8±0.3	27				
BeO(E)	90	1-3/8	0	1-3/8	B	1.9±0.3	21				
						1.9±0.3	24				
BeO(F)	90	1-3/8	0	1-3/8	B	1.9±0.3	23				
	U^{238} Detector		Np^{237} Detector					$M_{st}(U^{238})$	$M_{st}(Np^{237})$	$M_{eff}(U^{238})$	$M_{eff}(Np^{237})$
BeO(A)	90	1-17/32	0	1-17/32	--	<0.1	negligible	1.59	1.85	1.59	1.85

Notes: Cup = Cup surrounding U^{235} detector
Angle = Angle between detector and incident deuteron beam
Distance = Distance from center of target to front end of detector

reflector (Figs. 8, 15) indicates that the average energy of the delayed neutrons is of the order of 1 kev. Evidence for such a low energy component for WC and a higher energy for U was also found in the analysis of the neutron spectrum emerging from critical assemblies of U^{235} reflected first with WC and then with U (LA-258). These transmission measurements (LA-258), using 95% B^{10} absorbers of varying thickness, indicated that for the U reflector no part of the emerging neutron spectrum was below 0.1 Mev, whereas 2% of the spectrum from the WC reflector could be attributed to 1.5-kev neutrons.

At thermal energy, the probability of capture of neutrons in a BeO reflector is of the order of 5% of the probability of leakage, and it is even smaller at higher energies. Therefore one can consider the BeO reflector as just a scattering medium for which the diffusion theory can be applied. The mean lifetime, τ_a, measured in this case is

$$\frac{1}{\tau_a} = \frac{1}{\tau_\ell} = \frac{\pi^2}{3NR^2}\frac{v}{\sigma_{tr}} = \frac{\pi^2 D}{R^2} \qquad (15)$$

The U^{235} fission-pulse-time distribution for BeO was obtained first with a cadmium and then with a boron cup surrounding the U^{235} chamber. The boron cup was 3/8" thick and had 0.0892×10^{24} atoms/cm^3 of B (normal isotopic

mixture). This cup would transmit (1/e)th of the neutrons having an energy of 90 ev. The lifetimes were obtained with the U^{235} detector at 0^{o} and 90^{o} to the incident beam to investigate whether there was any angular asymmetry. Within the experimental error, there was no observable angular dependence of the measured mean lifetimes.

For an approximate calculation of the diffusion constant for BeO, (density = 2.1 gm/cm^3), the reflector is considered as a solid sphere and Eq. (15) is utilized. Using the value of $\tau_a = 4.4 \pm 1.5$ μsec for the neutron lifetime as measured with the U^{235} detector surrounded with a cadmium cup, the diffusion constant $D = (2.4 \pm 0.6) \times 10^6$ cm^2/sec, which corresponds to a transport cross section of (5.3 ± 2) barns at an average energy of 45 ev. The average energy of 45 ev was chosen because the pulse-time distribution curves indicate that 46% of the fissions delayed are in the energy range 0.22 to 90 ev. For the energy range above 90 ev, the calculated diffusion constant, using the average value of $\tau_a = 1.9 \pm 0.3$ μsec, is (5.6 ± 0.9) x 10^6 cm^2/sec, which corresponds to a transport cross section of (3.2 ± 0.5) barns at 90 ev. These cross sections at 45 and 90 ev are reasonable considering that the thermal neutron scattering cross section for BeO is approximately 8 barns.

C. Growth Curve for the Neutrons in the Reflector.

For a rectangular source, the exponential growth of the number of detected U^{235} fissions is

$$F(t) = F_o (1 - e^{-t/\tau}) \qquad 0 \leq t \leq T \tag{16}$$

and the exponential decay of the detected fission after the source of neutrons is turned off is

$$F(t) = F(T) \cdot e^{-(t - T)/\tau}, \qquad t \geq T \tag{17}$$

The rectangular pulse indicated in Fig. 21 would be the shape of F(t) if τ were infinitesimal. F_o is the saturation value of the detected fissions if the source were left on for a long time instead of being turned off at time t = T. F(T) is the number of fissions detected at time T when the neutron source is turned off.

For the source of neutrons obtained from the modulated D-D source, if there were no observable decay constant τ for the neutrons in the reflector, the fission-pulse-time curve would have the same shape and duration as the bare source fission-pulse-time curve given by Eq. (4). When there is an observable neutron mean lifetime τ, the growth of the fission-pulse curve can be calculated by considering the source function, $F_o(t)$, as being made up of a large number of rectangular sources of width Δt (Fig. 22). The ordinate, F(t), of the growth curve at time $t = k\Delta t$ is the

sum of the ordinates at time t of the decay curves of the preceding k - 1 rectangular source elements of width Δt plus the ordinate of the growth curve of the k^{th} rectangular source element.

$$F(t) = F_o(t)(1 - e^{-\Delta t/\tau}) + \sum_{j=0}^{k-1}\left[F_o(j\cdot\Delta t)(1 - e^{-\Delta t/\tau})e^{-(t-j\cdot\Delta t)/\tau}\right] \tag{18}$$

where τ is the time constant for the exponential growth curve. The first term in Eq. (18) is the k^{th} term of the series in Eq. (18). Therefore

$$F(t) = \sum_{j=0}^{k}\left[F_o(j\cdot\Delta t)(1 - e^{-\Delta t/\tau})e^{-(t-j\cdot\Delta t)/\tau}\right] \tag{19}$$

if

$$\frac{\Delta t}{\tau} \ll 1, \qquad e^{-\Delta t/\tau} = 1 - \frac{\Delta t}{\tau} \tag{20}$$

Substituting Eq. (20) in Eq. (19)

$$F(t) = \sum_{j=0}^{k}\left[F_o(j\cdot\Delta t)e^{-(t-j\cdot\Delta t)/\tau}\cdot\frac{\Delta t}{\tau}\right]$$

Let $j\cdot\Delta t = t'$ (t' is the running variable). Since Δt is uniform, $\Delta t = \Delta t'$, and

$$F(t) = \lim_{\Delta t' \longrightarrow 0}\sum\left[F_o(t')e^{-(t - t')/\tau}\cdot\frac{\Delta t'}{\tau}\right]$$

$$\therefore F(t) = \frac{1}{\tau}\int_{t'=0}^{t'=t}\left[dt'F_o(t')e^{-(t-t')/\tau}\right]$$

or

$$F(t) = \frac{e^{-t/\tau}}{\tau}\int_{t'=0}^{t'=t}\left[dt'F_o(t')e^{t'/\tau}\right] \tag{21}$$

($e^{-t/\tau}$ is taken out of the integral since t' is the variable).

The differential equation of the growth curve is obtained by differentiating Eq. (21)

$$\frac{dF(t)}{dt} = \frac{F_o(t) - F(t)}{\tau} \tag{22}$$

Proof: $$\frac{dF(t)}{dt} + \frac{F(t)}{\tau} = e^{-t/\tau} \cdot \frac{d(F.e^{t/\tau})}{dt} = \frac{F_o(t)}{\tau}$$

$$F(t)e^{t/\tau} = \int_o^t \frac{F_o(t')}{\tau} e^{t'/\tau} dt'$$

or

$$F(t) = \frac{e^{-t/\tau}}{\tau} \int_o^t dt' \cdot F_o(t')e^{t'/\tau}$$

It is interesting to note that if $F_o(t)$ is a rectangular function($\sqcup\sqcap\sqcup$)then Eq. (21) and Eq. (22) reduce to the familiar form of

$$F(t) = F_o (1 - e^{-t/\tau}) \tag{23}$$

and

$$\frac{dF(t)}{dt} = \frac{F_o - F(t)}{\tau} \tag{24}$$

The expression $F_o(t)$ in Eq. (21) would be the fission-pulse-time curve if τ were infinitesimal, and is given by the equation

$$F_o(t) = F\left(\frac{T}{2}\right)\sin^4\left(\frac{\pi t}{T}\right) \tag{4}$$

Equation (21) is valid for the time interval 0 to T (T = duration of modulated source). After the source is turned off, the decay of the pulse of neutrons is given by the exponential decay equation

$$F(t) = F(T)e^{-(t - T)/\tau}, \qquad t \geq T \tag{25}$$

where

$$F(T) = \frac{e^{-T/\tau}}{\tau}\int_0^T F_o(t')e^{t'/\tau}\, dt'$$

One might, off hand, think that if the source function is known and the value of the decay constant is measured from the slope of the ln F(t) vs t curve after the source is turned off, one might calculate the shape of the rise curve by the use of Eq. (21), which is easily integrable. This would be valid if there were only one value of τ while the source of neutrons is on. Any arbitrary distribution of neutrons in a reflector can be represented as a linear combination of normal modes, analagous to the modes of vibration of a vibrating string, (LA-29, CLASSIFIED). These normal modes have the property that the shapes of the normal mode distribution do not change with time, but only the amplitudes vary, either exponentially increasing or decreasing. The time behavior of this arbitrary distribution of neutrons can be understood in terms of the exponential rise or decay of its constituent normal modes. The

particular distribution of neutrons with which we are concerned could be thought of as being composed of these normal modes. Each mode has its particular value of τ for the reflector, and after the source of neutrons is turned off, the fundamental mode (largest τ) would persist, the higher modes dying out much more rapidly. The τ_a measured by investigating the exponential decay curve is the τ of the fundamental mode. This value of τ_a cannot be used to predict the rise of the pulse-time distribution curve because there are superimposed on the fundamental mode the higher modes, which have a much shorter lifetime. Therefore the rise of the experimental curve F(t) vs t would be faster than that predicted using the τ for the fundamental mode (Fig. 23). This was checked and found to be the case.

D. Effective Multiplication of the Reflectors.

In addition to determining τ_a, it is possible to measure the percentage of U^{235} fissions that are delayed, in spite of the complicated rise of curve B of Fig. 23. For a rectangular source function, the fissions delayed would be the shaded area A, or the shaded area B, (A = B), of Fig. 24. For a source function which is not rectangular in shape but of the form $F_o(t) = F(T/2) \sin^4 (\pi t/T)$, the fissions that are delayed are either shaded area a or b, (a = b), in Fig. 25. Curve I of Fig. 25 is the pulse-time

distribution curve as measured with the U^{235} fission chamber. Curve II of Fig. 25 would represent the pulse-time distribution curve, if the decay constant τ_a were infinitesimal (i.e., if none of the U^{235} fissions are delayed by a time greater than the resolving time of the pulse-time analyzer, 10^{-7} sec). The shape and duration of curve II are known from the U^{238} fission-pulse-time distribution curves obtained with the bare source and with a reflector surrounding the source. The U^{235} fission-pulse-time distribution curves obtained with the bare source are also a measure of the shape and duration of curve II, $(F_o(t))$. If the area A under curve I is measured, then $F_o(T/2)$ (the maximum of the curve $F_o(t)$) may be determined, as curves I and II must have the same area underneath them.

$$\text{Area under Curve I} = A = \int_o^T dt \cdot F_o\left(\frac{T}{2}\right) \sin^4\left(\frac{\pi t}{T}\right)$$

$$A = \left(\frac{3}{8}\right) F_o\left(\frac{T}{2}\right) \cdot T, \qquad \text{or } F_o(T/2) = (8/3)\, A/T \tag{26}$$

In the evaluation of the data, the total area A under curve I is measured with a planimeter. $F_o(T/2)$ is then calculated using Eq. (26), and curve II is drawn. Area a or b is measured with the planimeter, and the fraction of U^{235} fissions delayed, f, is calculated:

$$f = \frac{a}{A} = \frac{b}{A} \tag{27}$$

Measurements of the neutron reflection of various materials have been carried out using a continuous source of neutrons (LA-304-CLASSIFIED). The multiplication, M, defined as the ratio of the average counting rate in the presence of a reflector to that for the bare source, was measured at the inner surface of the reflector, the same position at which all the modulation data was observed. The pulse-time analyzer is useful in determining the U^{235} fissions that are delayed more than 10^{-7} sec (the resolving time of the apparatus). The unshaded area, (A-a), of Fig. 25 is a measure of those U^{235} fissions which are delayed by less than 10^{-7} sec.

In view of the delayed U^{235} fissions, it is desirable to define an effective multiplication, (M_{eff}), of the reflector, taking into account only those U^{235} fissions which are delayed by less than 10^{-7} sec (the resolving time of the pulse-time analyzer). This multiplication is defined as the steady-state multiplication (M_{st}) times the factor (1 - f), where f is the fraction of U^{235} fissions delayed, Eq. (27).

$$M_{eff} = M_{st} (1 - f) = M \frac{(A - a)}{A} \qquad (28)$$

The effective multiplication of the various reflectors was determined by measuring areas A and (A - a) with a

planimeter. Both steady-state and effective multiplication values are included in Table 1.

Figures 8, 10-12, (and Table 1) indicate the estimates of the percentage of U^{235} fissions delayed in the BeO and WC reflectors. For all reflector and core measurements, the U^{238} (or Np^{237}) data were normalized to the U^{235} data so that the U^{235} and U^{238} fission-pulse-time distribution curves have the same area underneath them. The normalization factor was the ratio of the integral U^{235} counts to the integral U^{238} (or Np^{237}) counts which were recorded by the scalers shown in Fig. 2. The neutron yield of the modulated source was monitored by counting the protons from the alternate D-D reaction. As in the bare source measurements, all data are taken for 1000 clicks of the proton monitor counter (64,000 proton counts). The ordinate on all the time distribution curves is fission counts / 1000 proton counts.

The percentage of the U^{235} fissions delayed by more than 10^{-7} sec for U was negligible (Fig. 7), whereas 13% of the U^{235} fissions were delayed more than 10^{-7} sec for WC (Fig. 8). This, in turn, means that the effective U^{235} multiplication of the U reflector is approximately 30% higher than the effective U^{235} multiplication of the WC reflector (5.4 for U as compared with 4.10 for WC).

The BeO reflector measurements are interesting in that 70% of the U^{235} fissions are delayed by more than 10^{-7} sec, yet the effective U^{235} and U^{238} multiplications are comparable to the effective U^{235} and U^{238} multiplications of the U (Table 1). Twenty-four percent of U^{235} fissions are delayed by more than 10^{-7} sec, as determined with a boron cup surrounding the U^{235} fission detector, which indicates that approximately 46% of the U^{235} fissions delayed are in the energy range 0.22 to 90 ev (the boron cup transmits (1^{th}/e) of the neutrons having an energy of 90 ev).

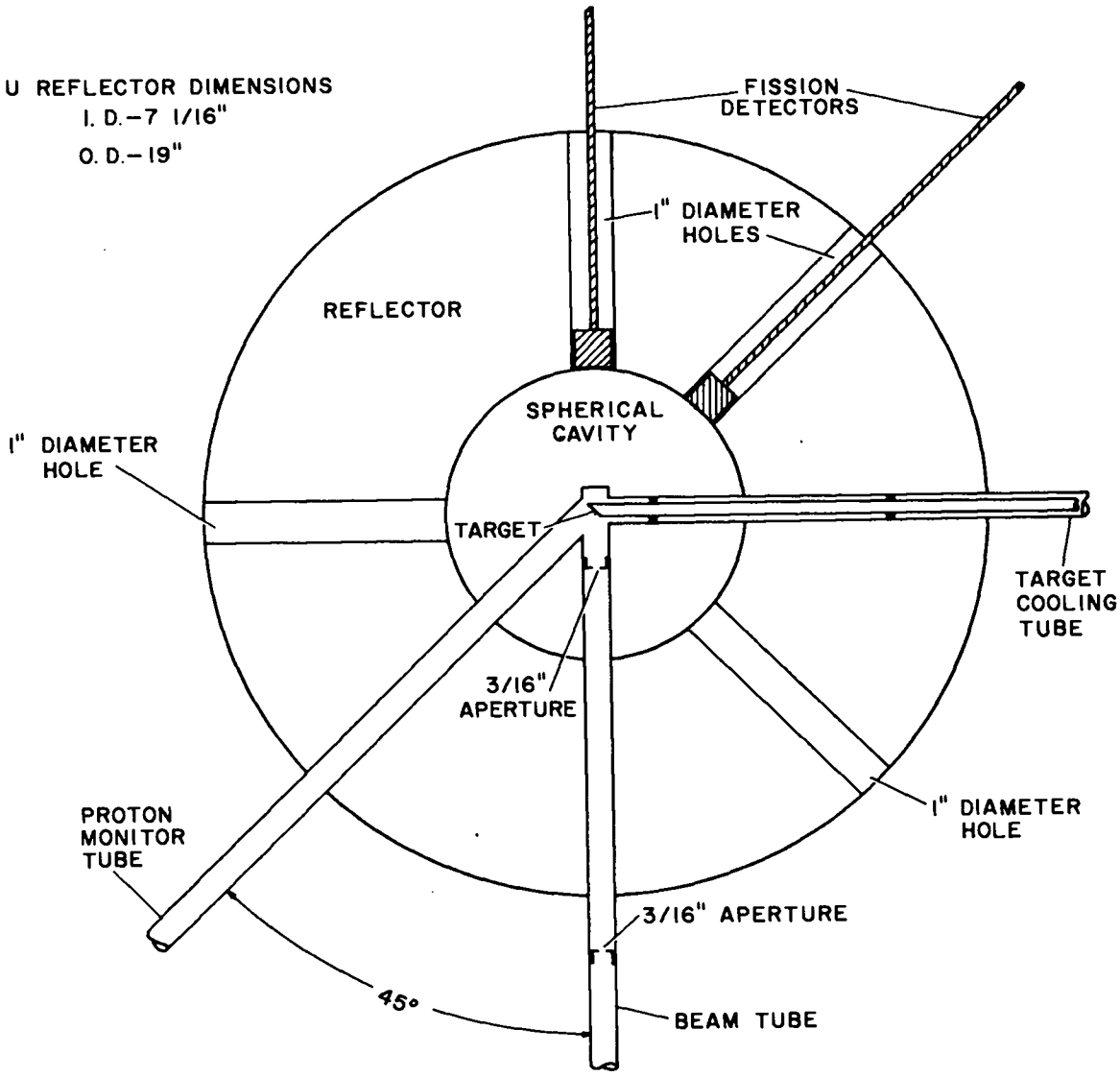

Figure 1. Experimental arrangement

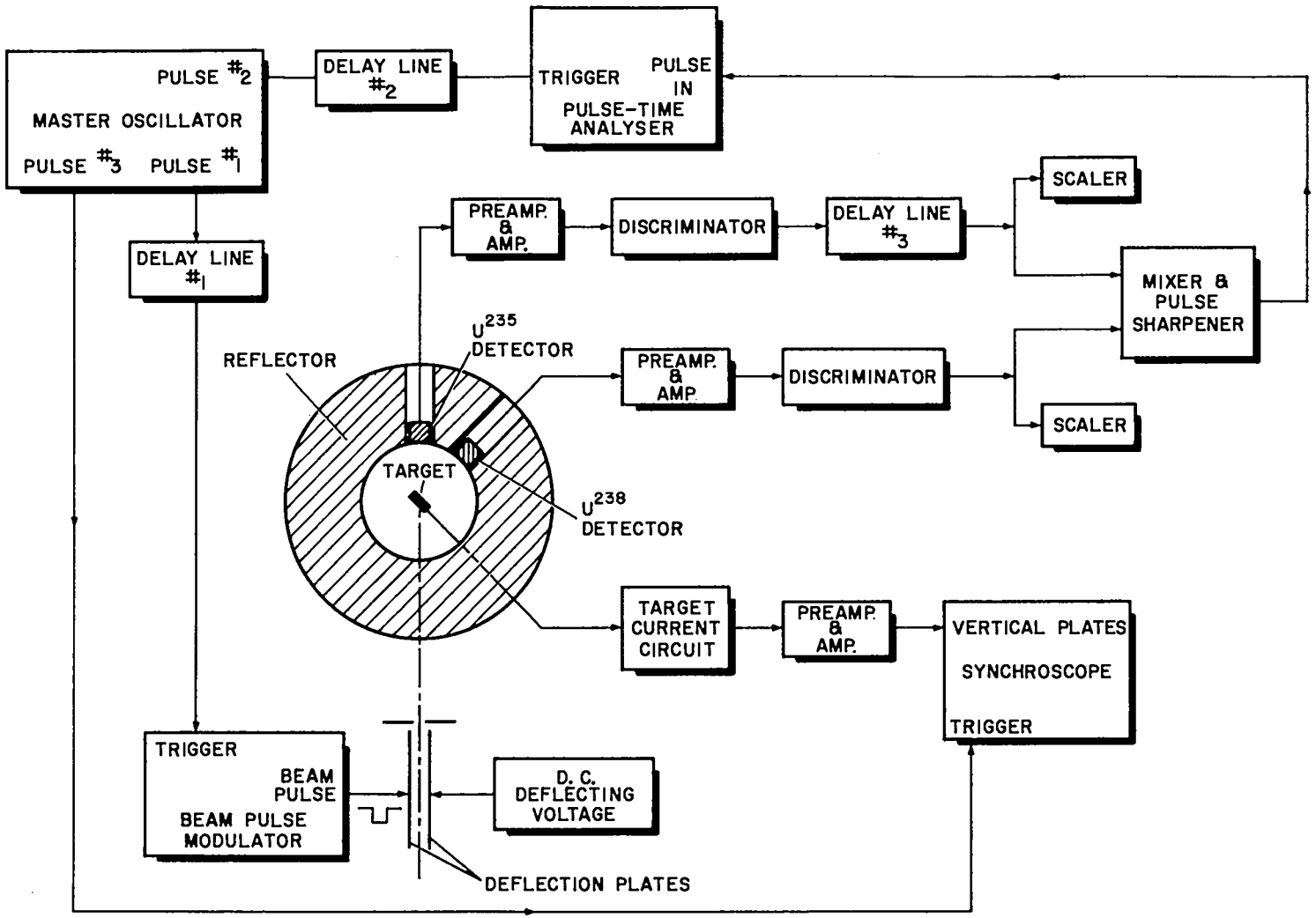

Figure 2. Detection system

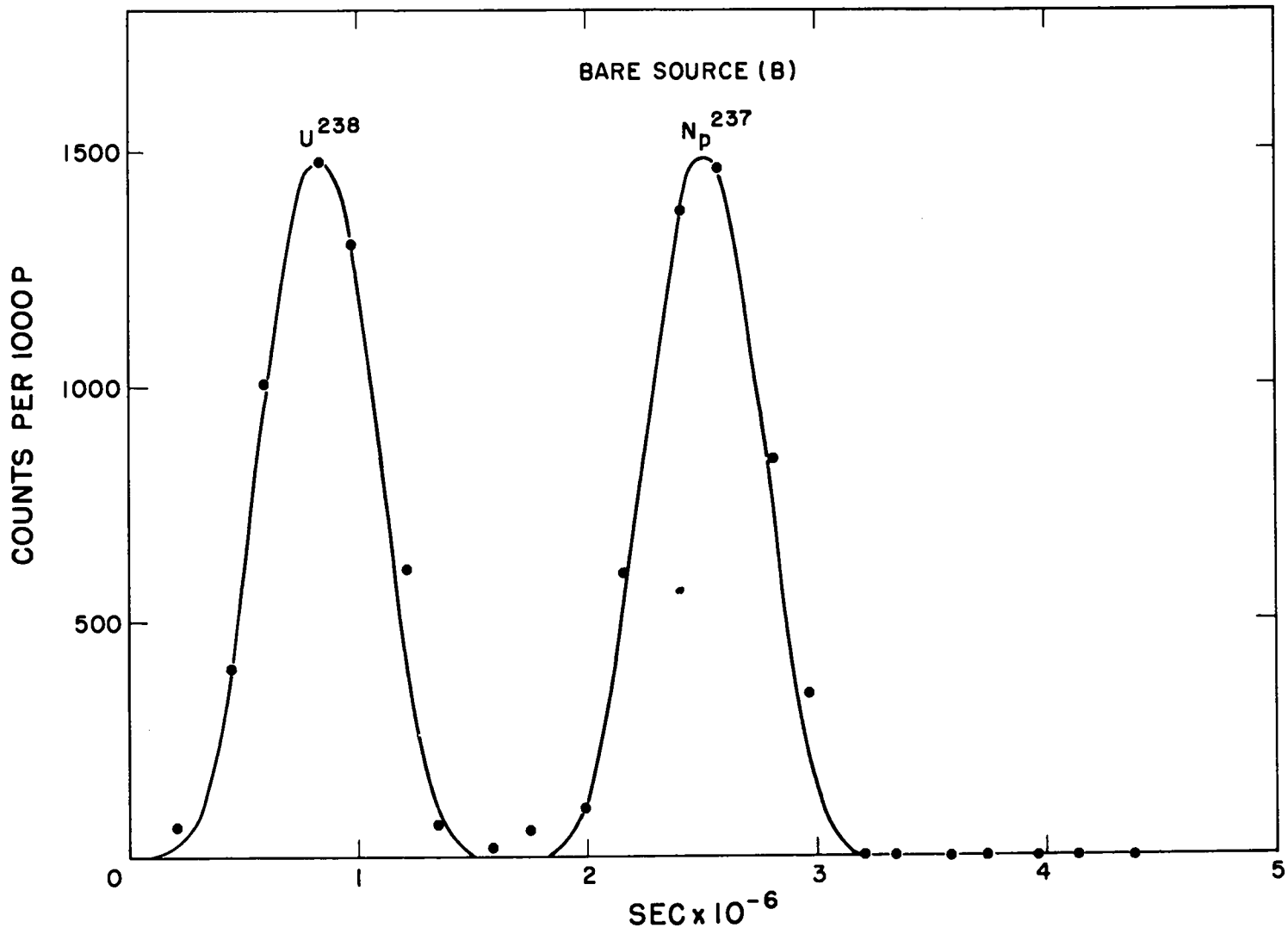

Figure 3. Time distribution of U^{238} and Np^{237} fissions. No reflector

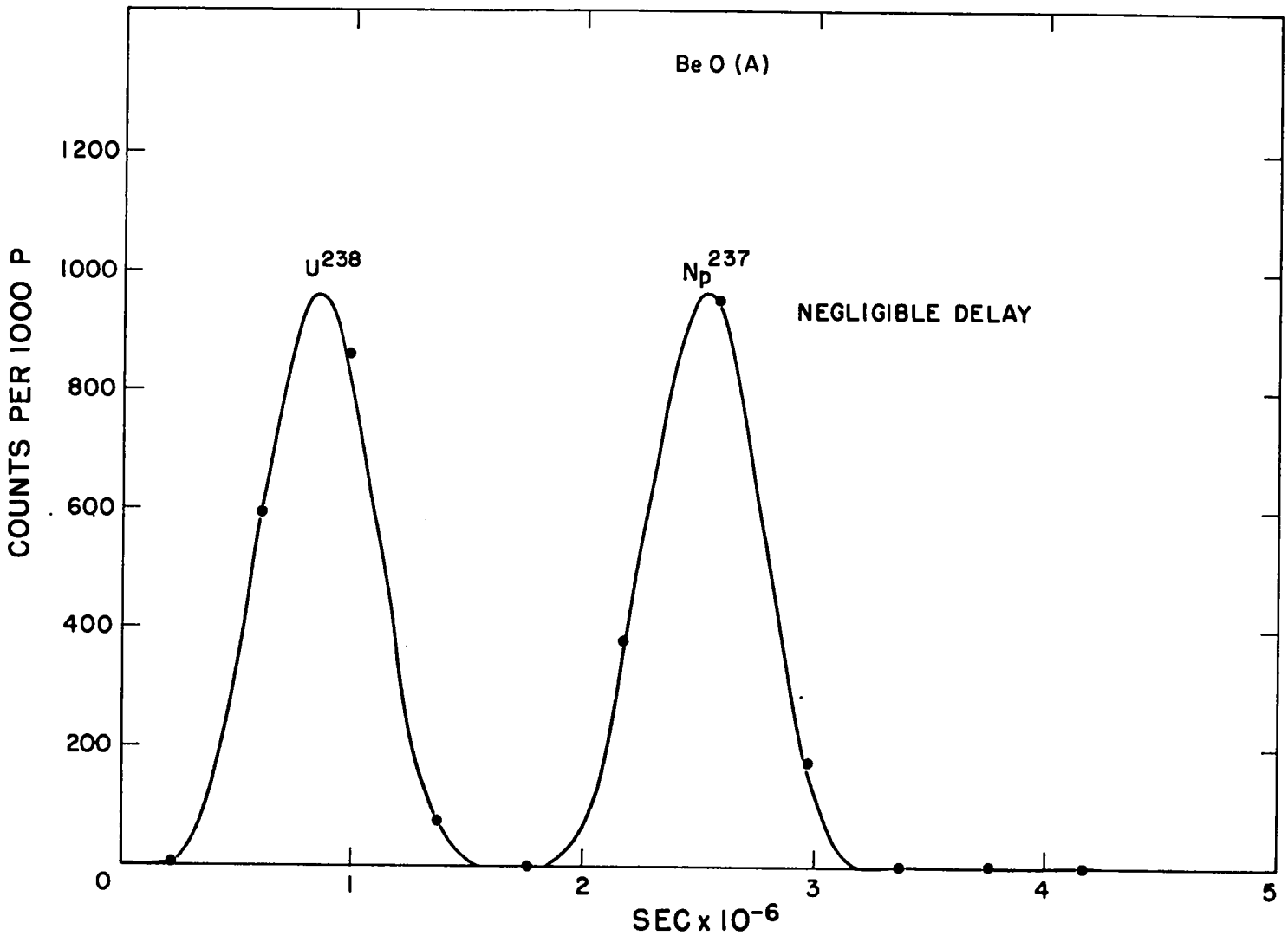

Figure 4. Time distribution of U^{238} and Np^{237} fissions. BeO reflector

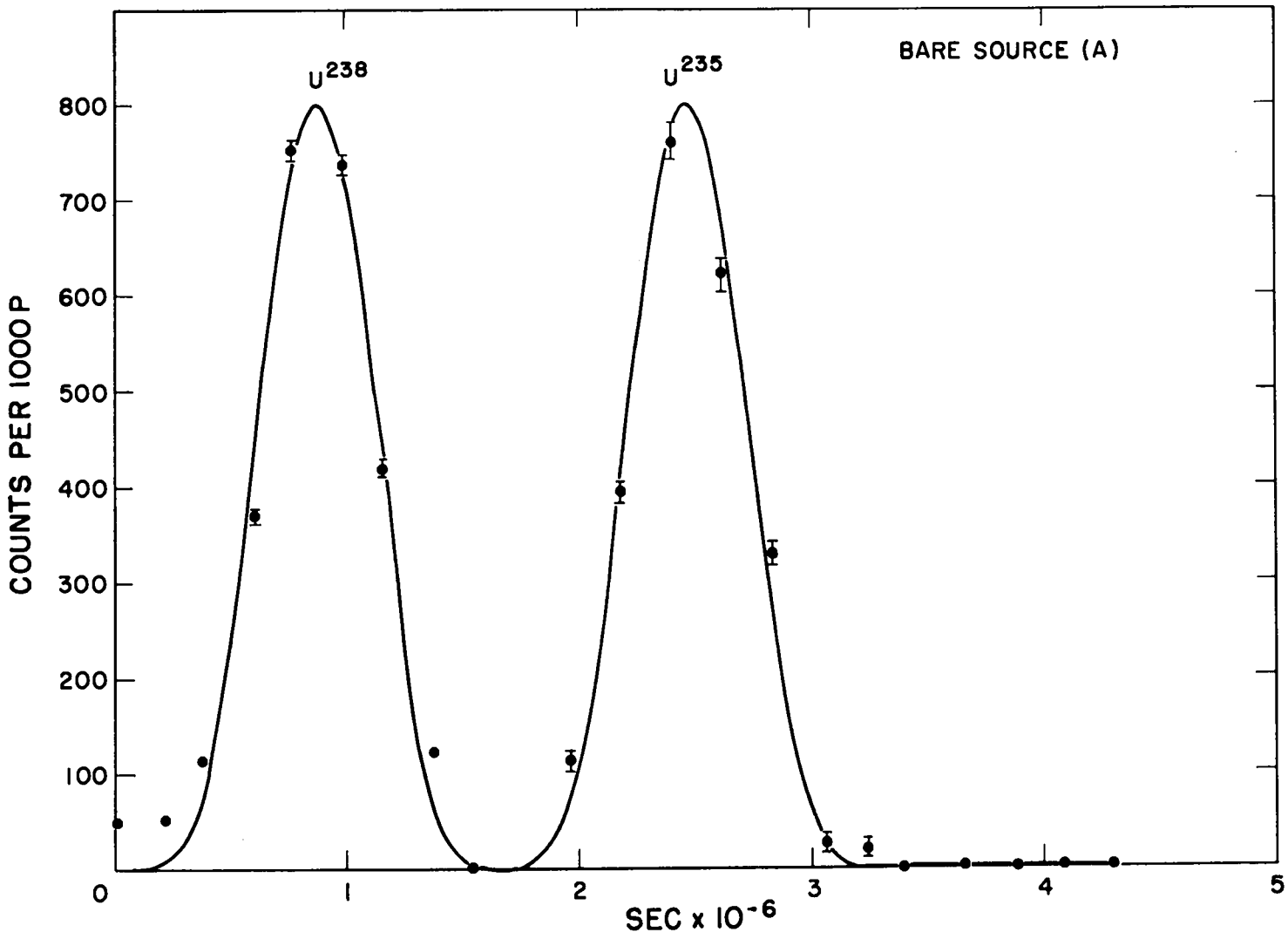

Figure 5. Time distribution of U^{238} and U^{235} fissions. No reflector

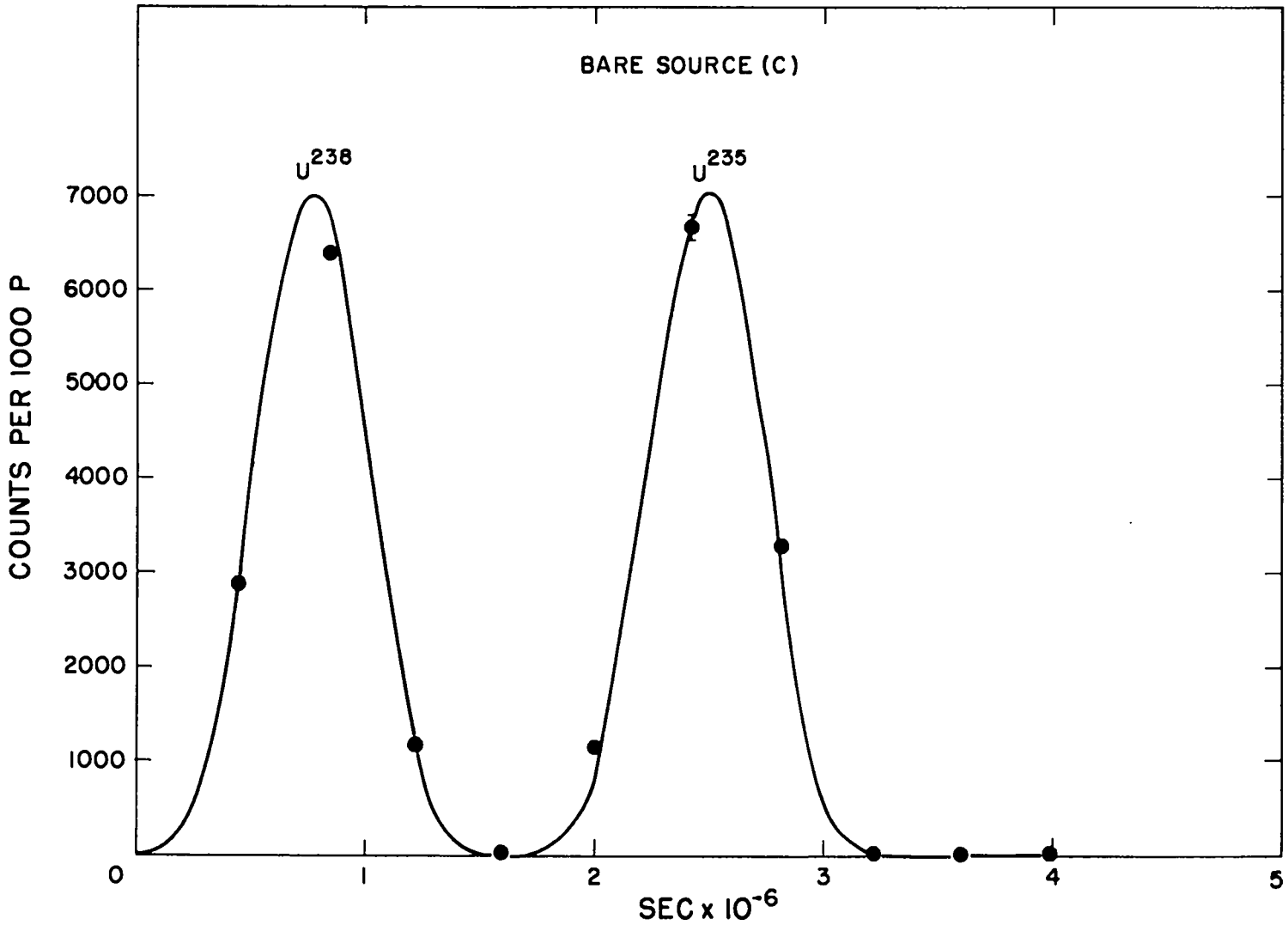

Figure 6. Repeated time distribution of U^{238} and U^{235} fissions. No reflector

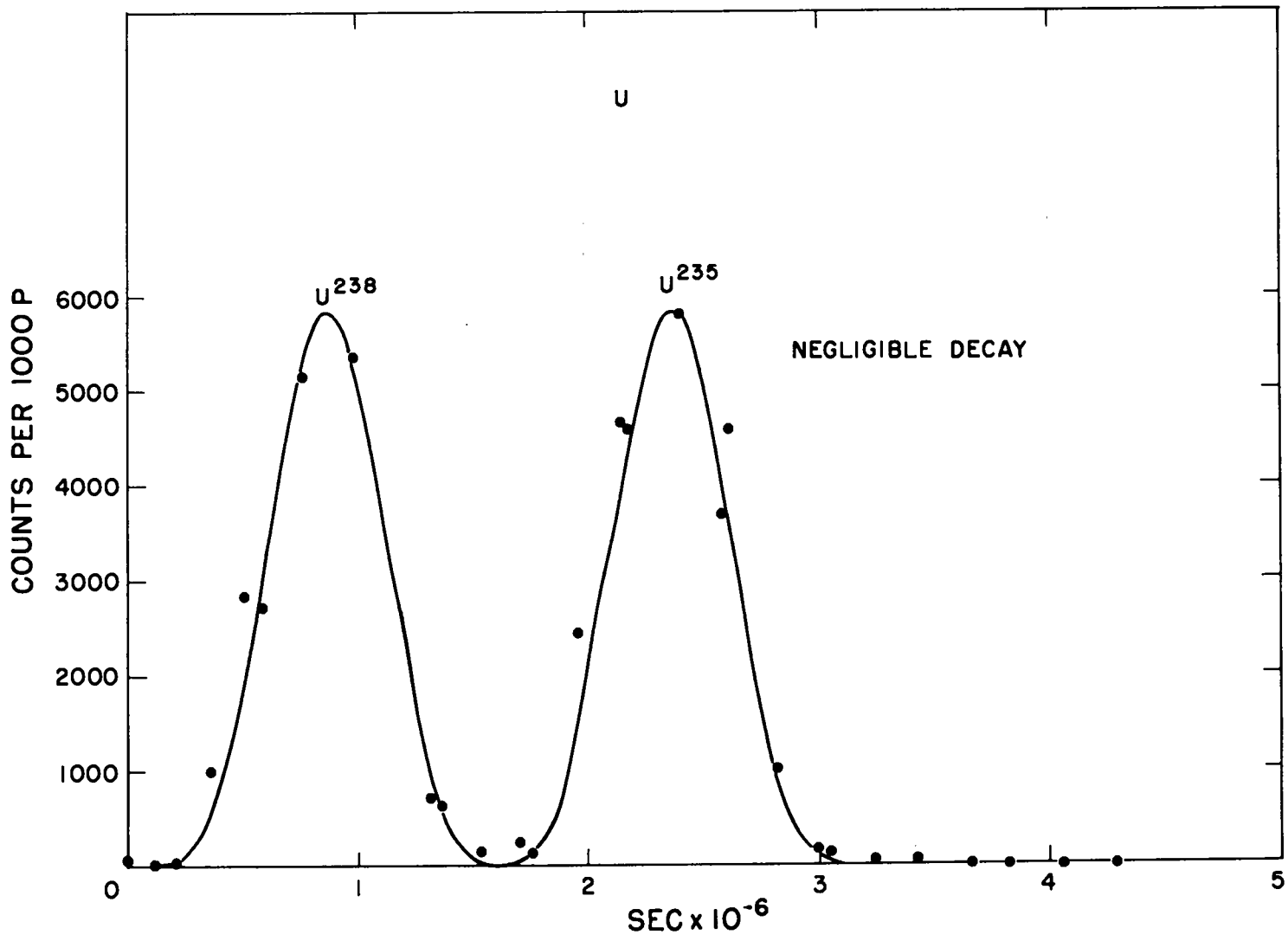

Figure 7. Time distribution of U^{238} and U^{235} fissions. U reflector

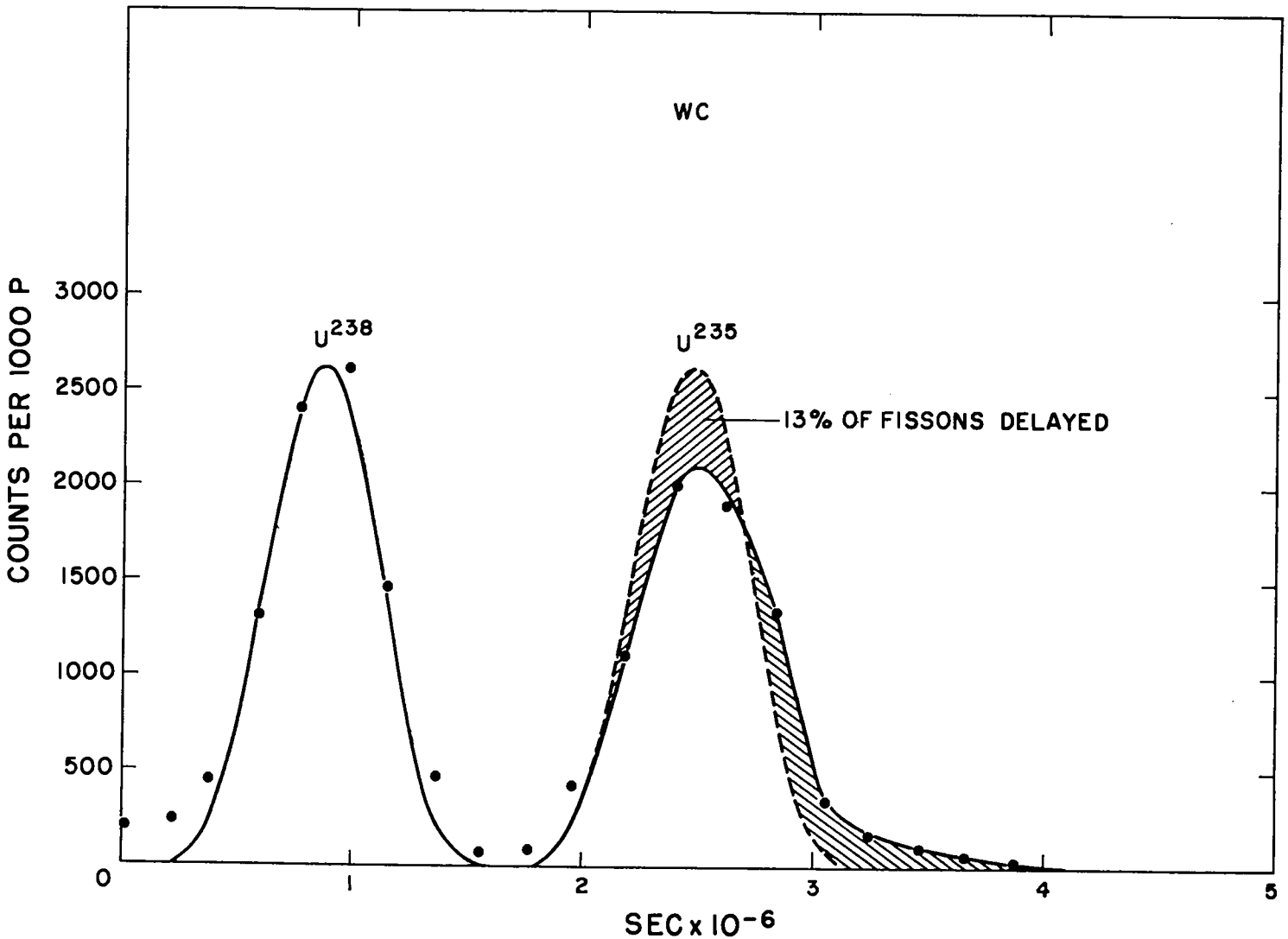

Figure 8. Time distribution of U^{238} and U^{235} fissions. WC reflector

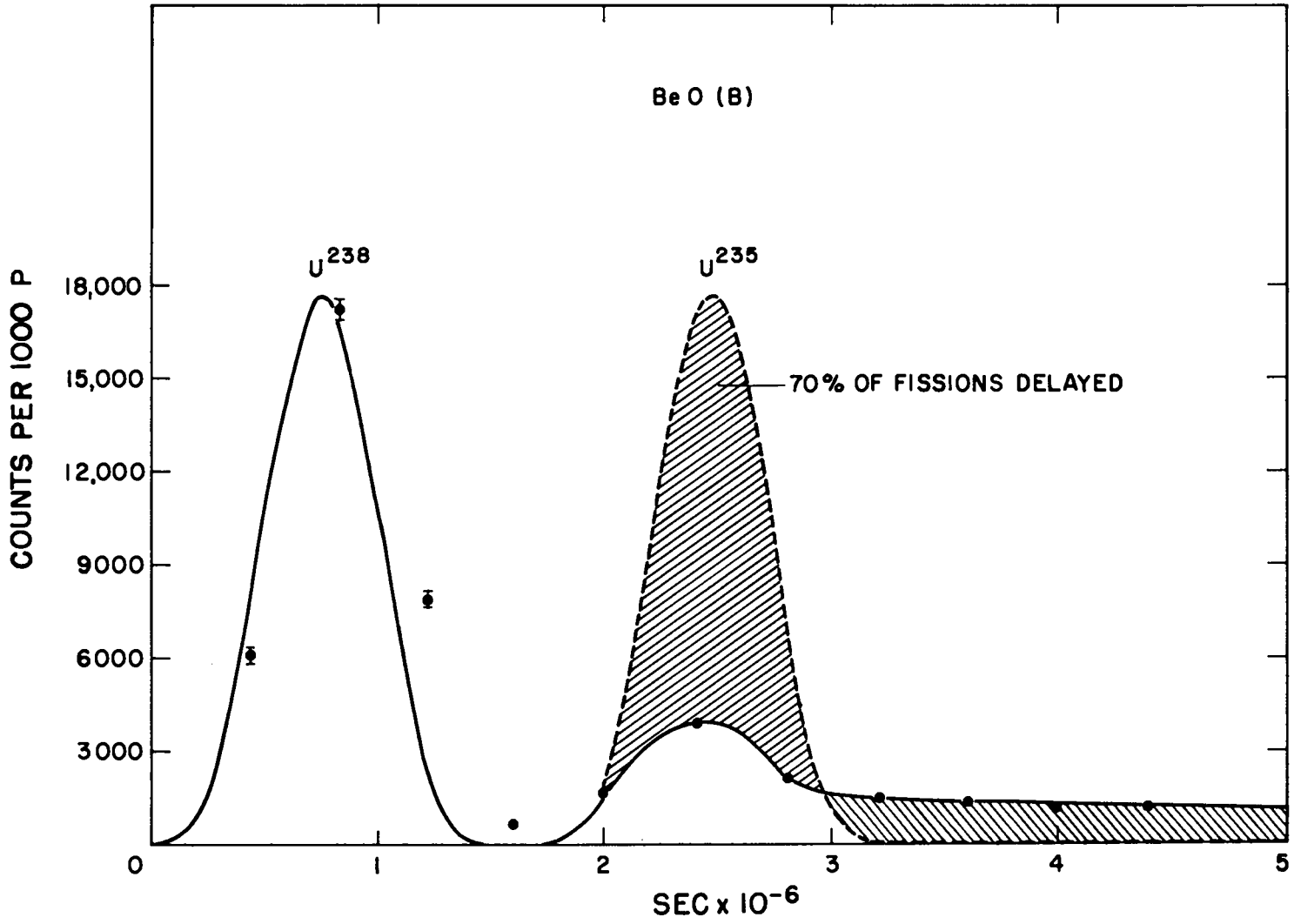

Figure 9. Time distribution of U^{238} and U^{235} fissions. BeO reflector, arrangement B of Table 1

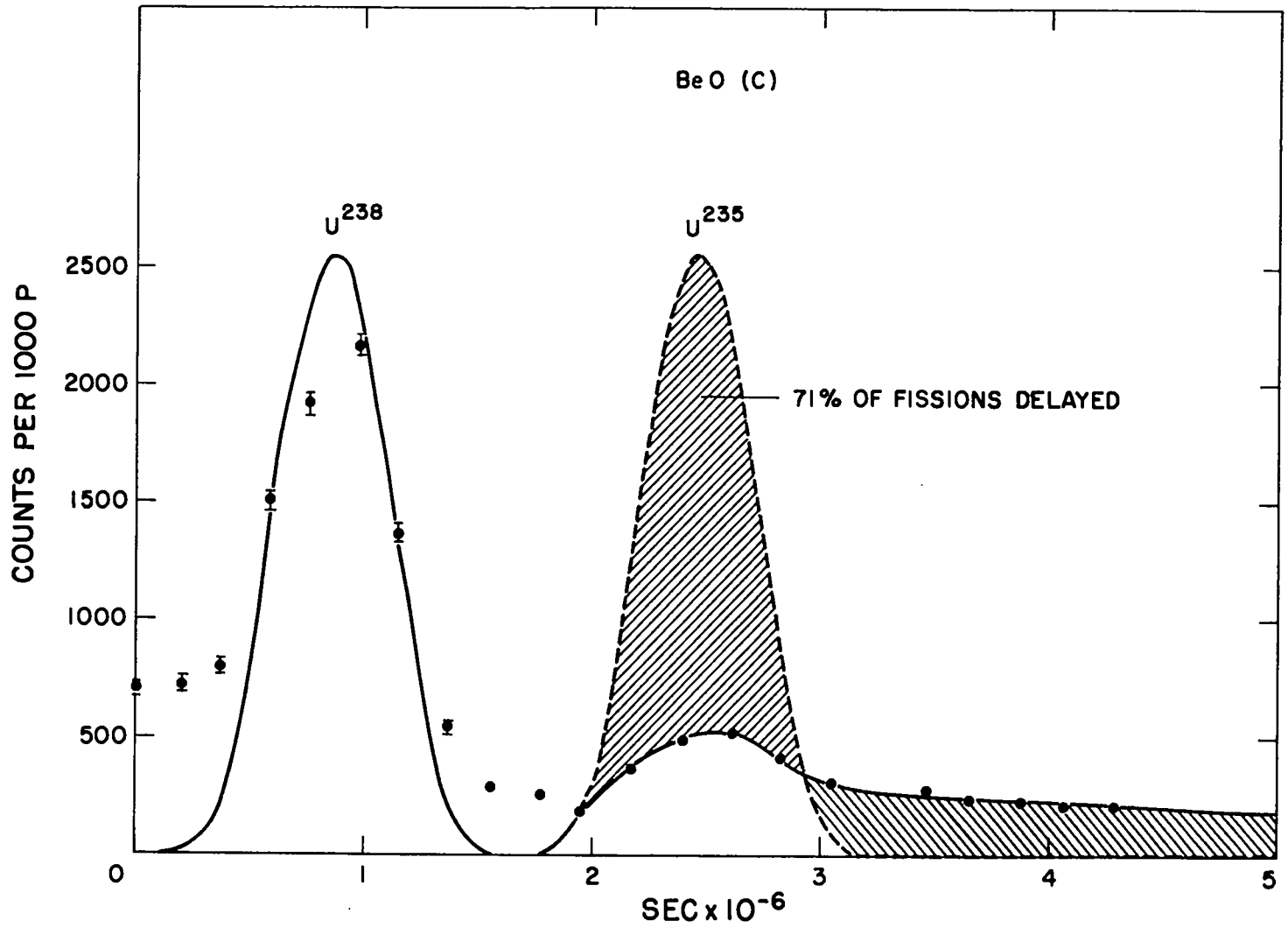

Figure 10. Time distribution of U^{238} and U^{235} fissions. BeO reflector, arrangement C of Table 1

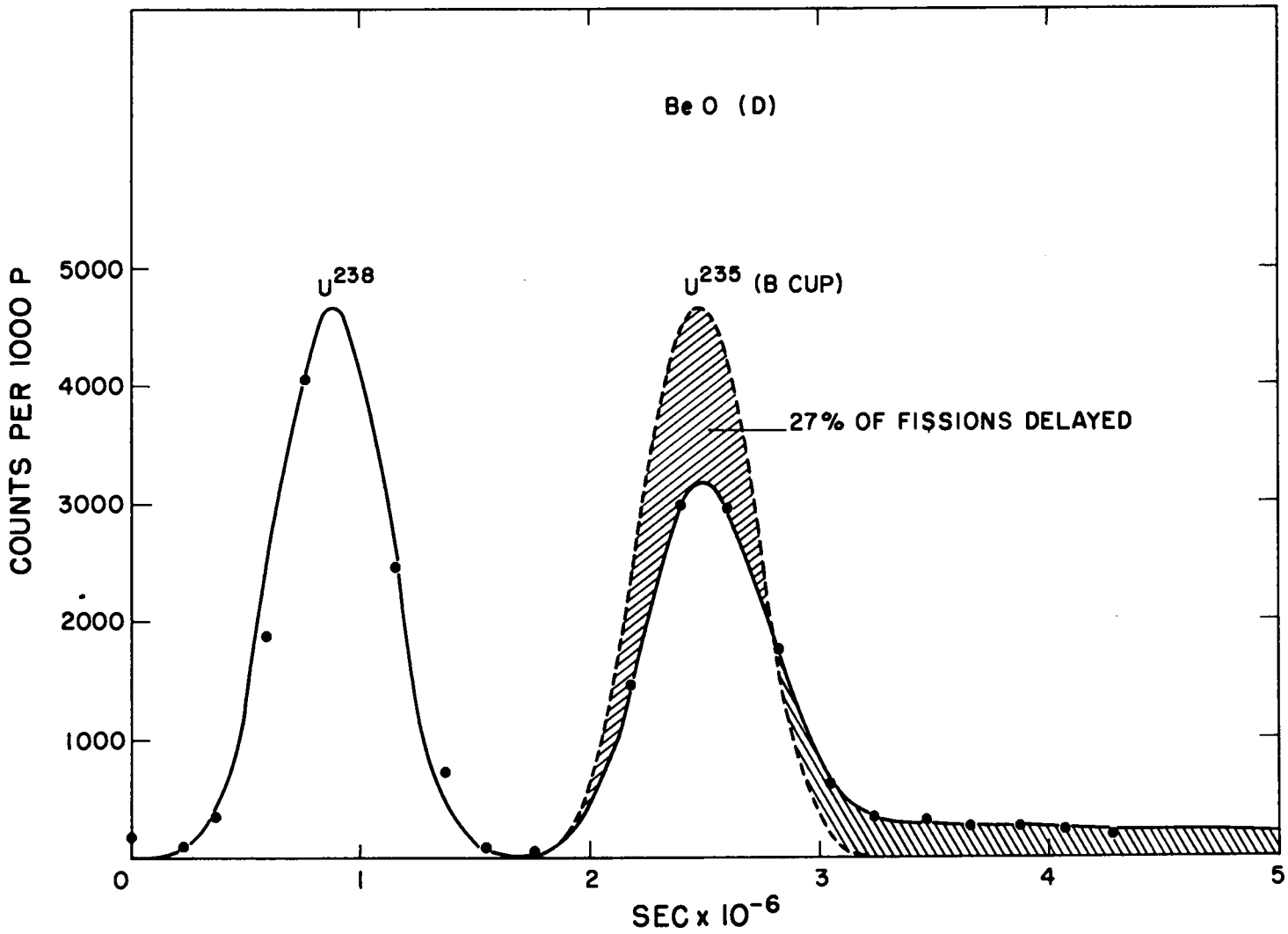

Figure 11. Time distribution of U^{238} and U^{235} fissions. BeO reflector, arrangement D of Table 1

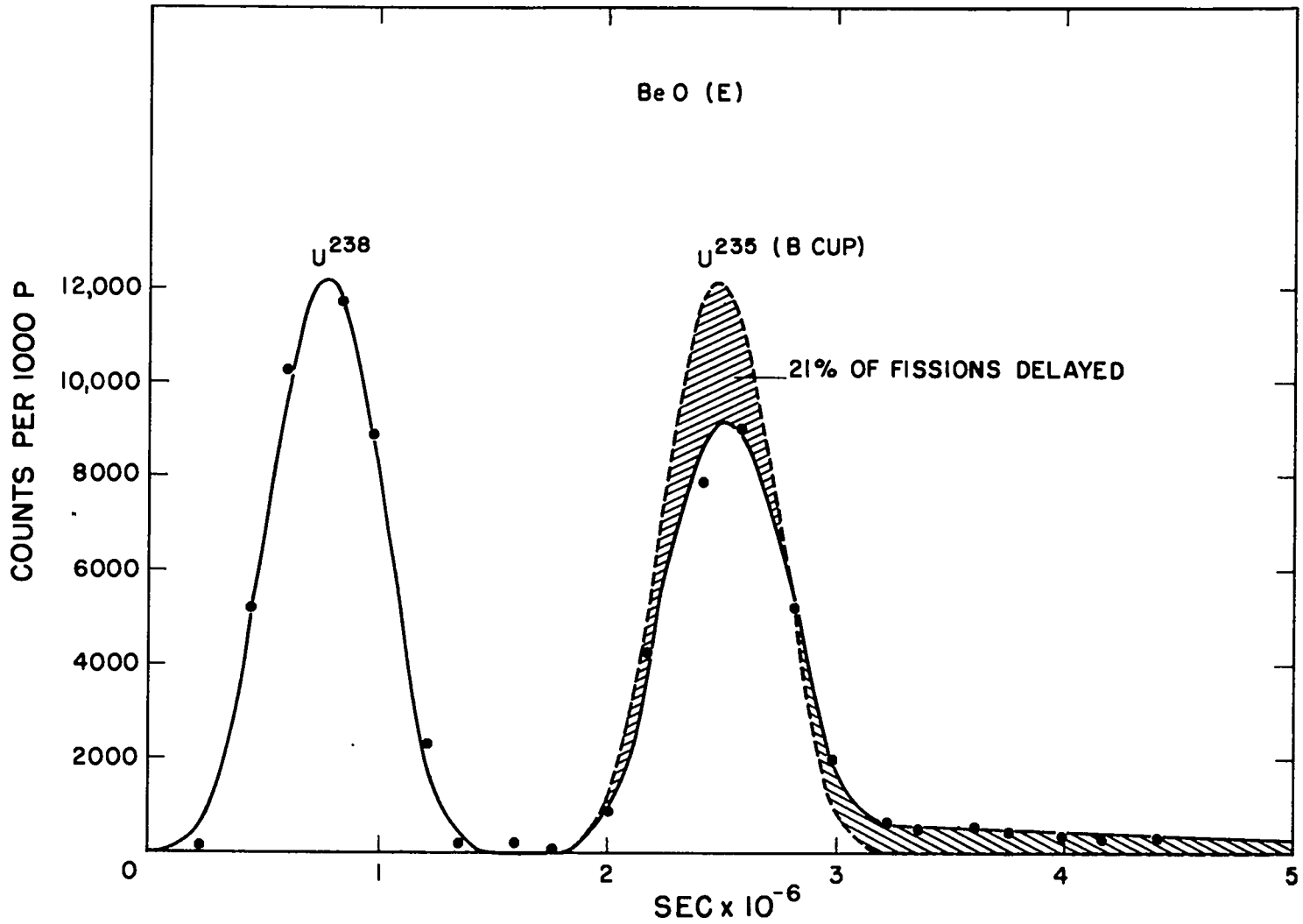

Figure 12. Time distribution of U^{238} and U^{235} fissions. BeO reflector, arrangement E of Table 1

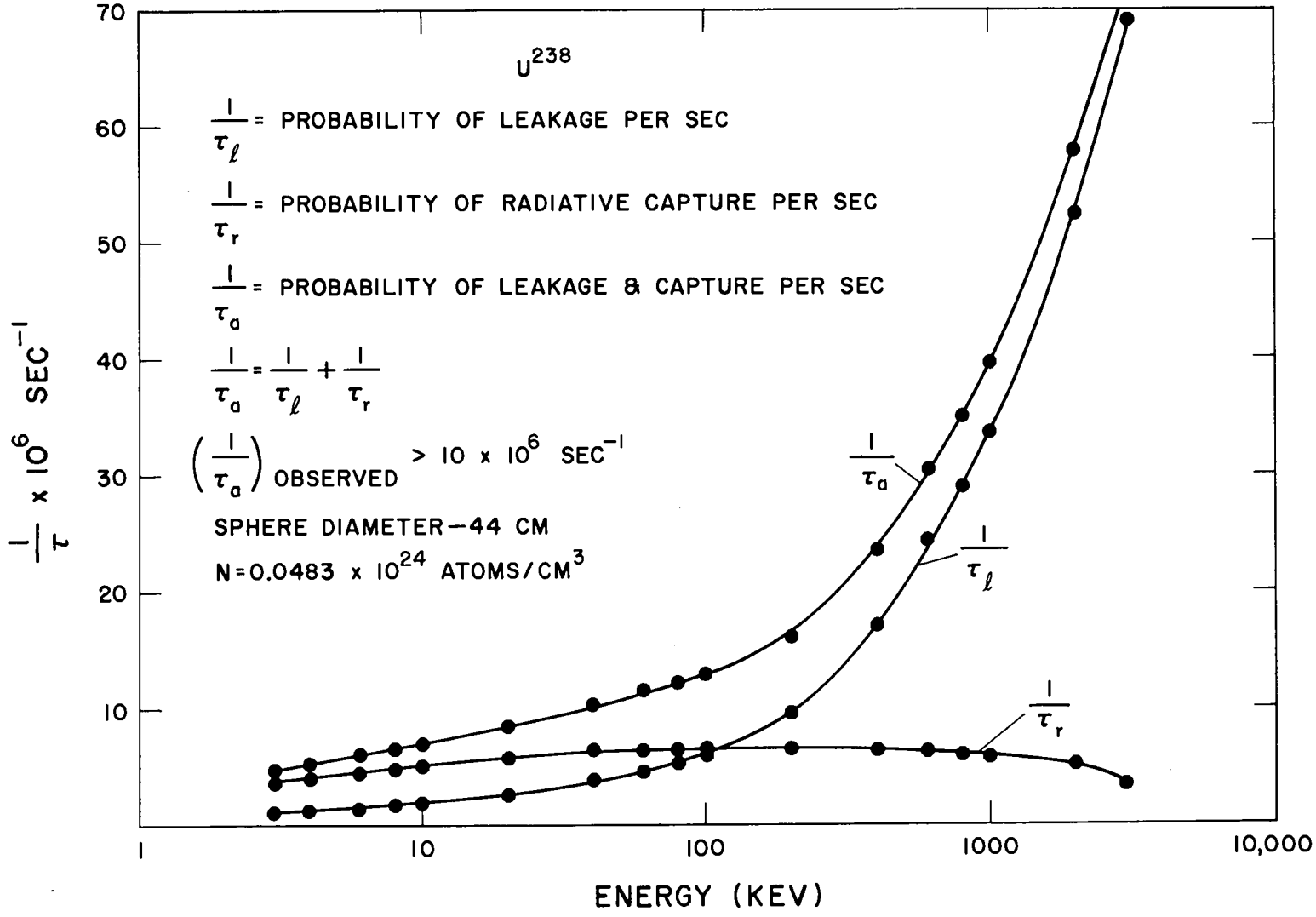

Figure 13. Dependence of leakage and capture probabilities upon neutron energy. U reflector

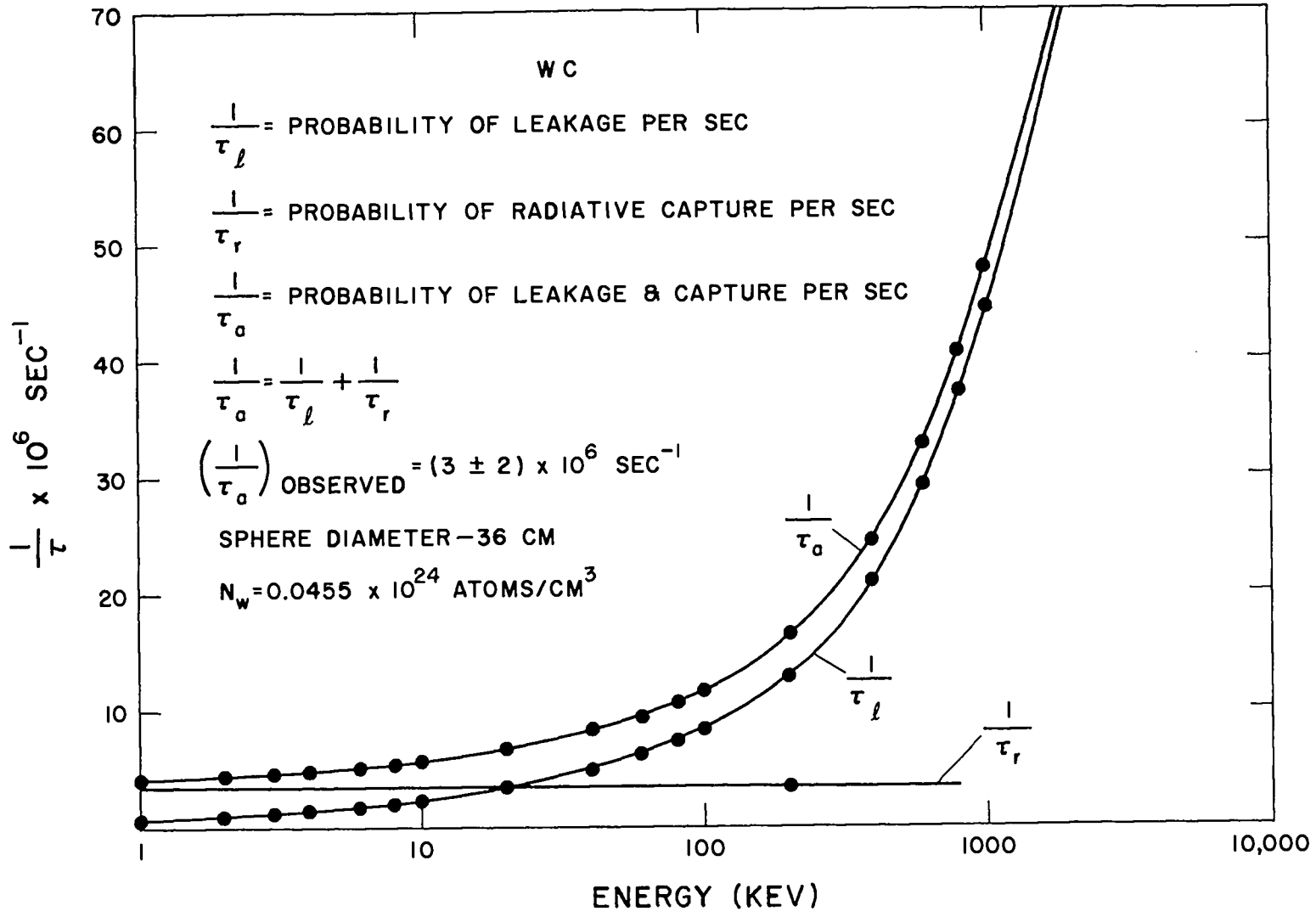

Figure 14. Dependence of leakage and capture probabilities upon neutron energy. WC reflector

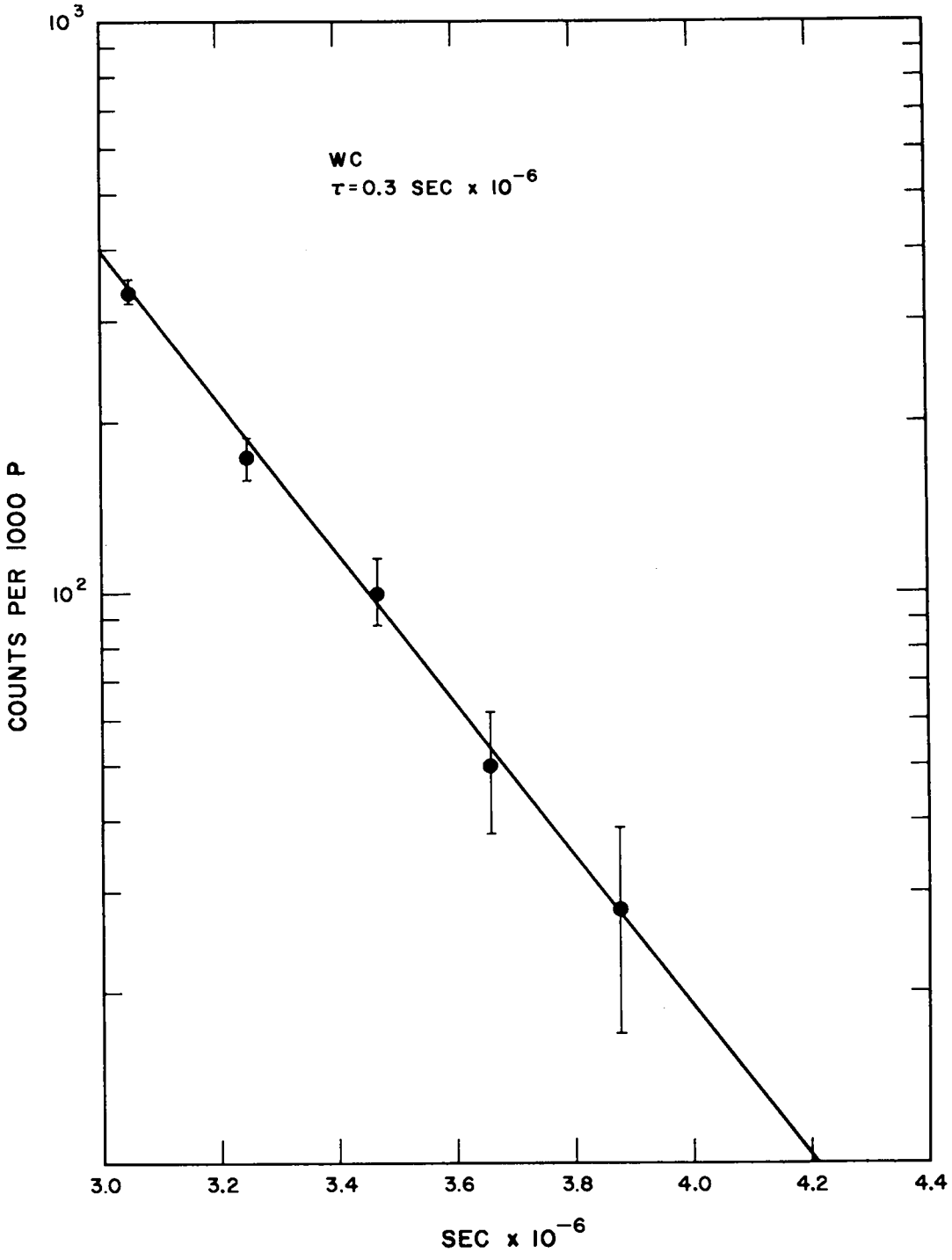

Figure 15. U^{235} fission decay in WC reflector

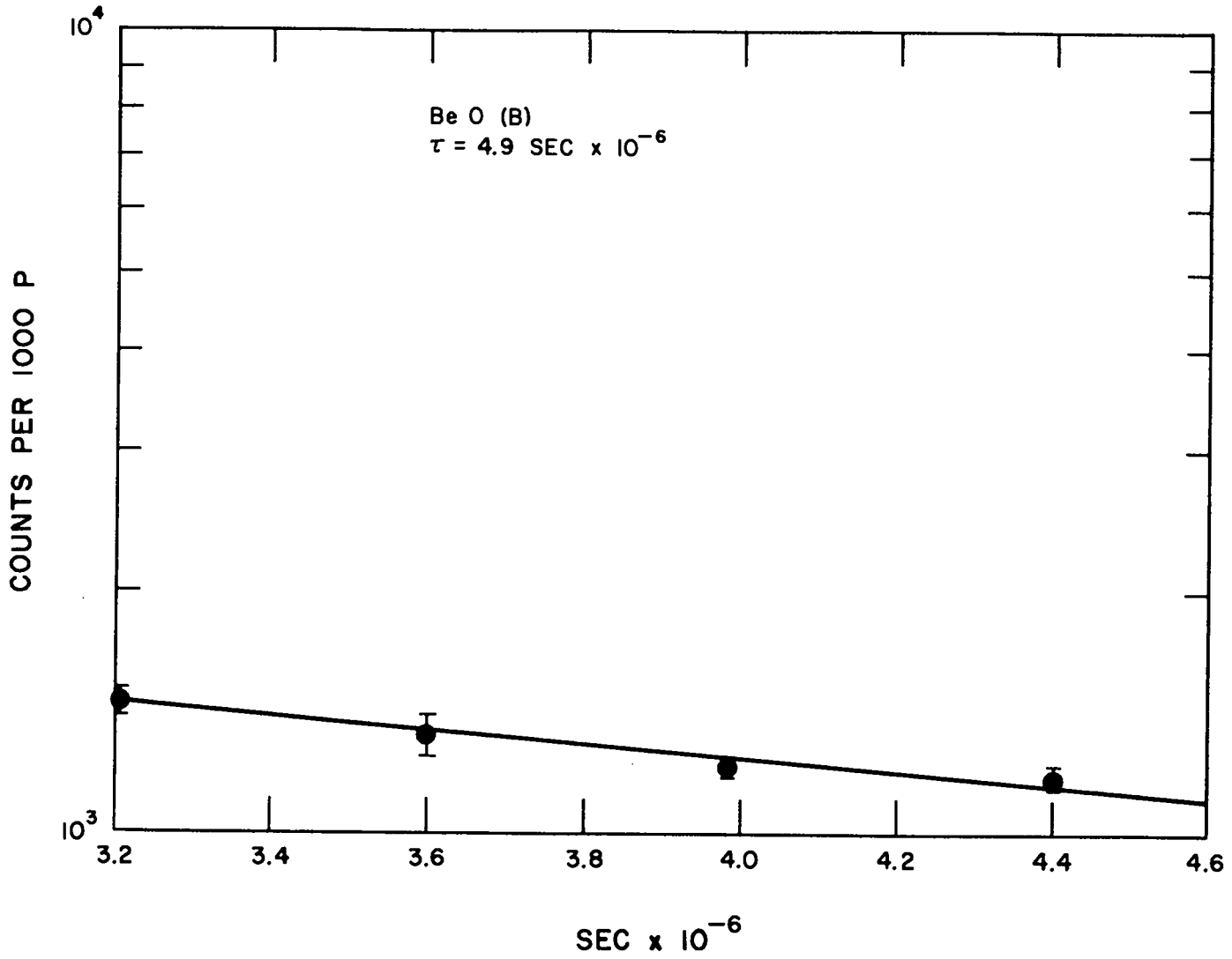

Figure 16. U^{235} fission decay in BeO reflector. Arrangement B of Table 1

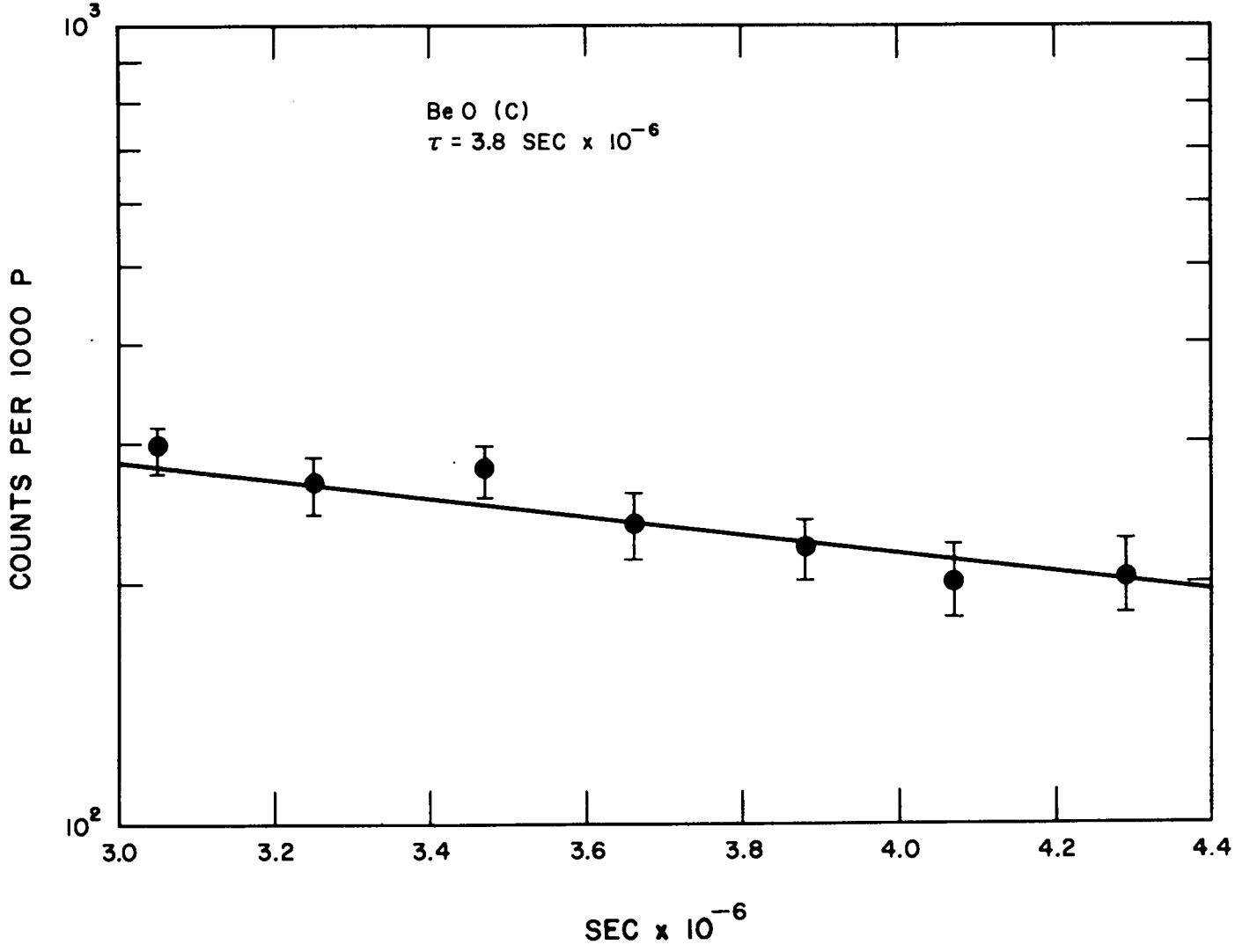

Figure 17. U^{235} fission decay in BeO reflector. Arrangement C of Table 1

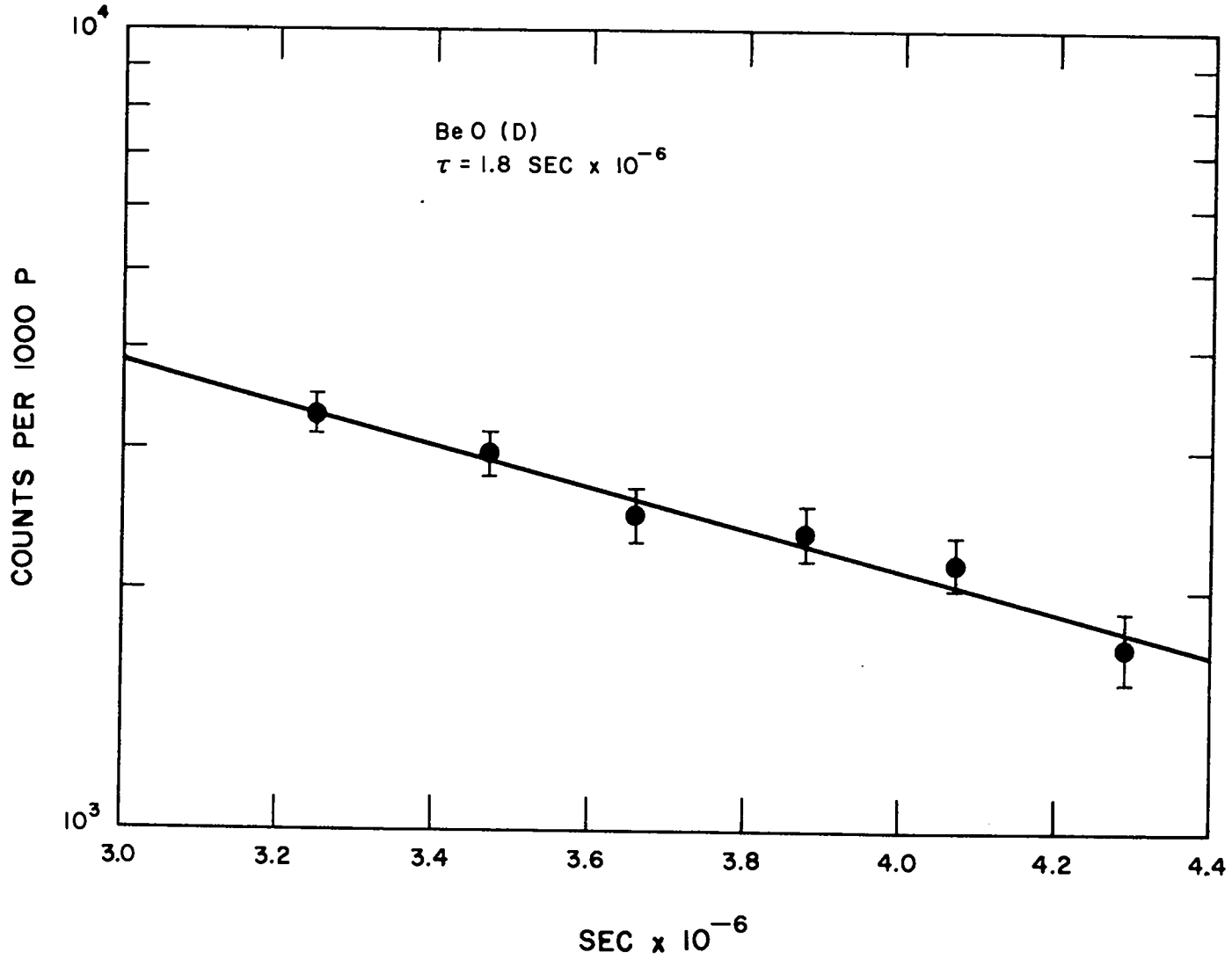

Figure 18. U^{235} fission decay in BeO reflector. Arrangement D of Table 1

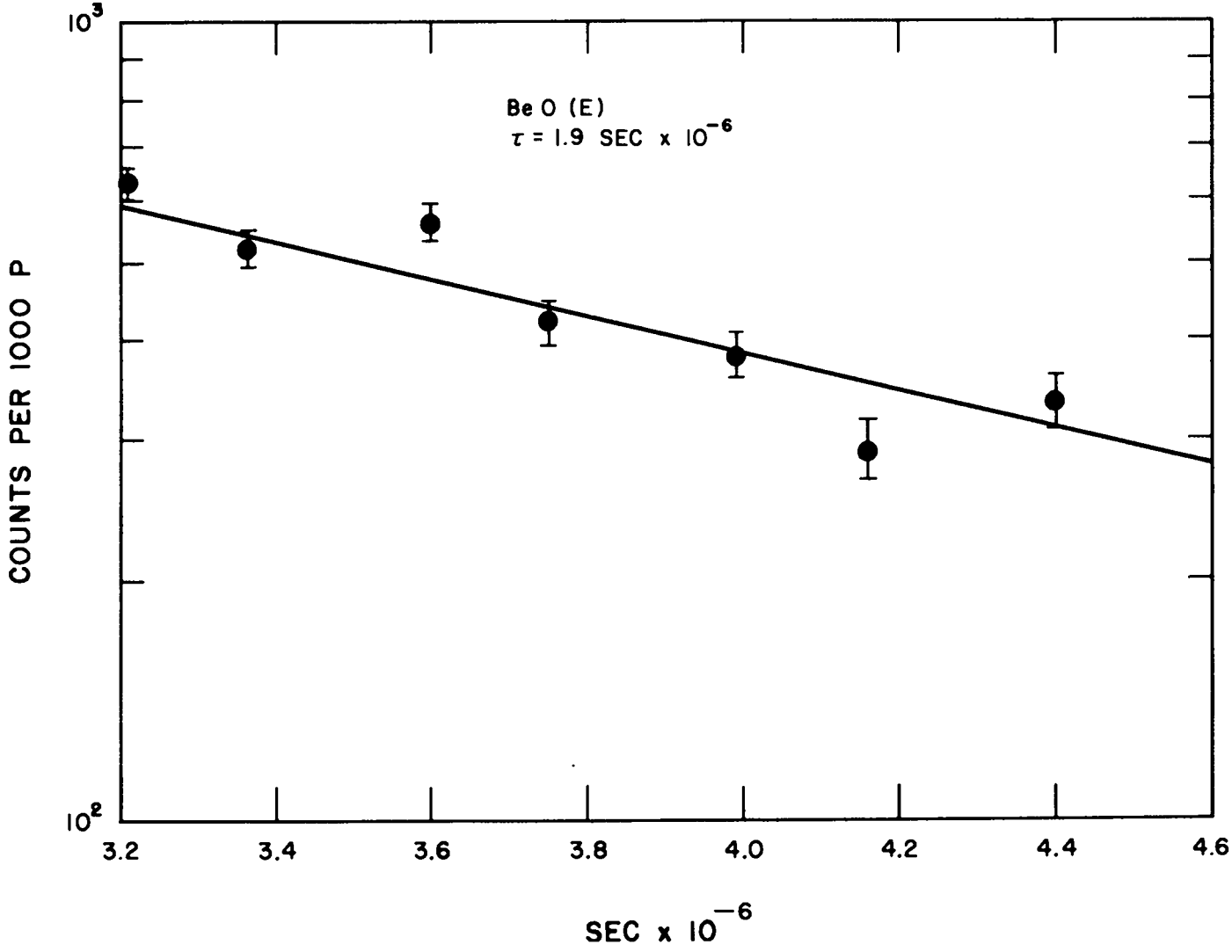

Figure 19. U^{235} fission decay in BeO reflector. Arrangement E of Table 1

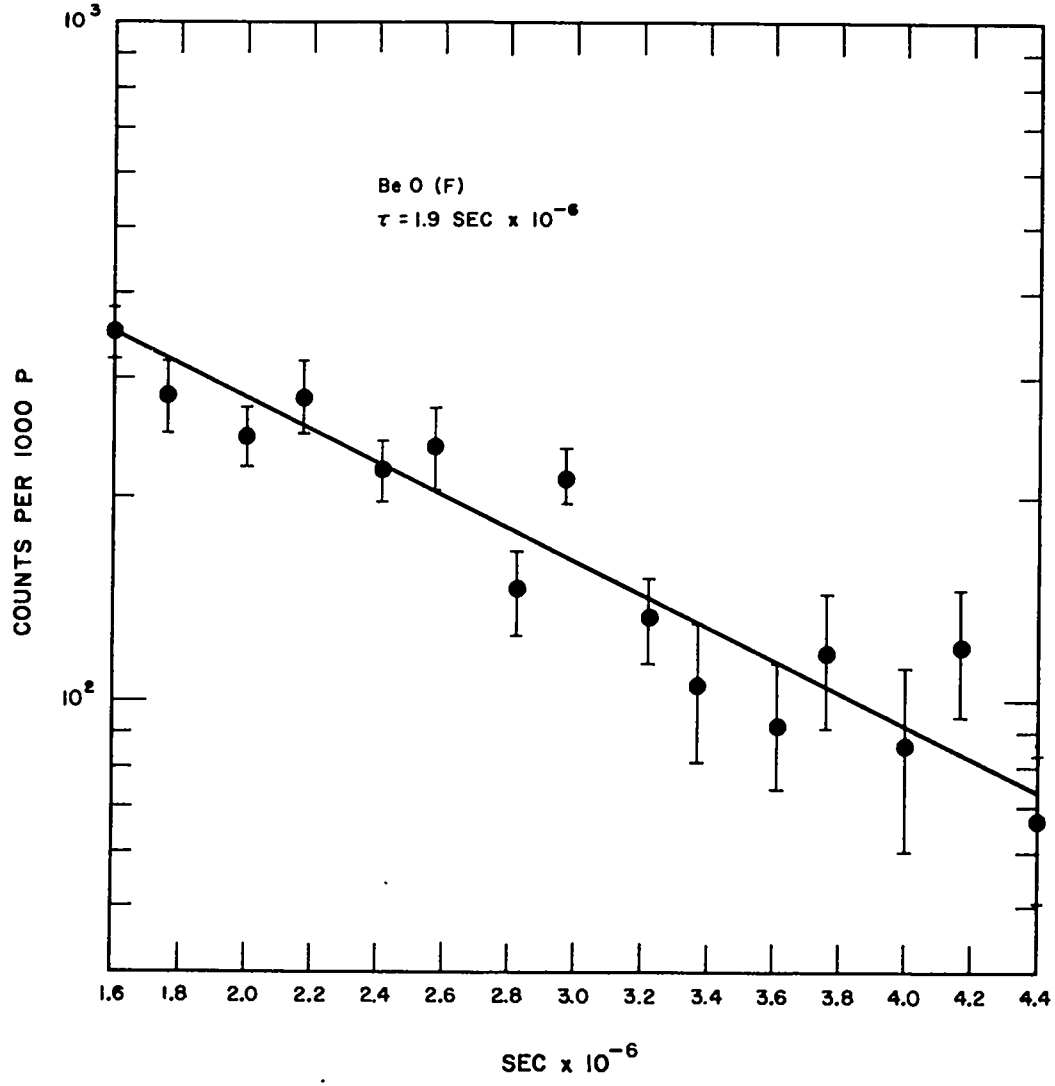

Figure 20. U^{235} fission decay in BeO reflector. Arrangement F of Table 1

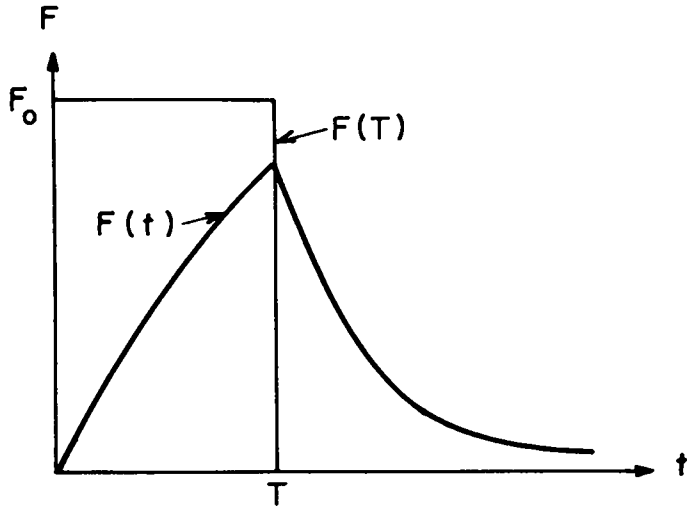

Figure 21. Response to rectangular source pulse if neutron decay constant is zero

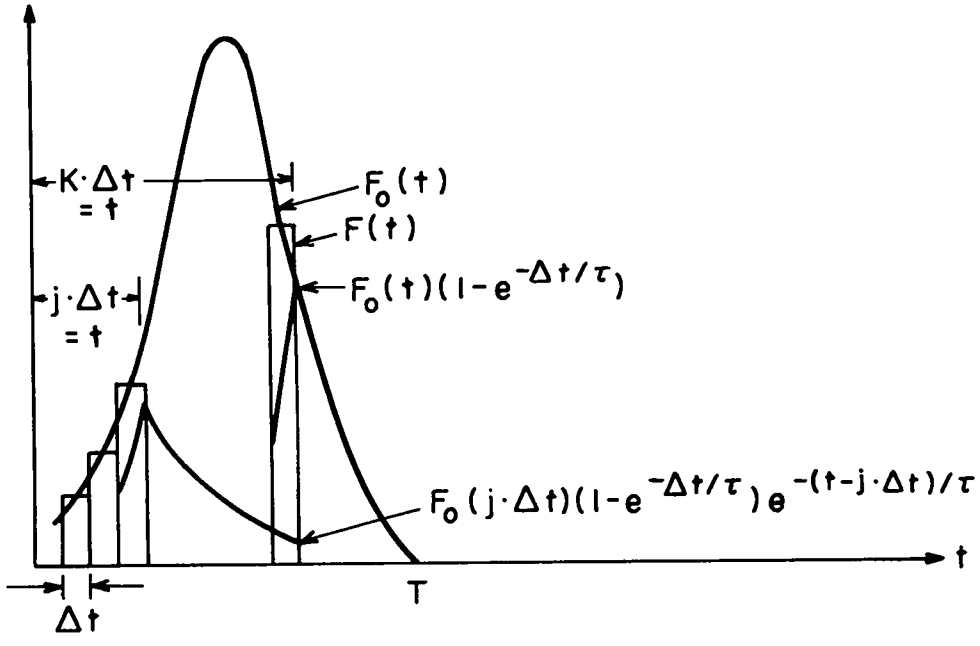

Figure 22. Response to source pulse if neutron decay constant is significant

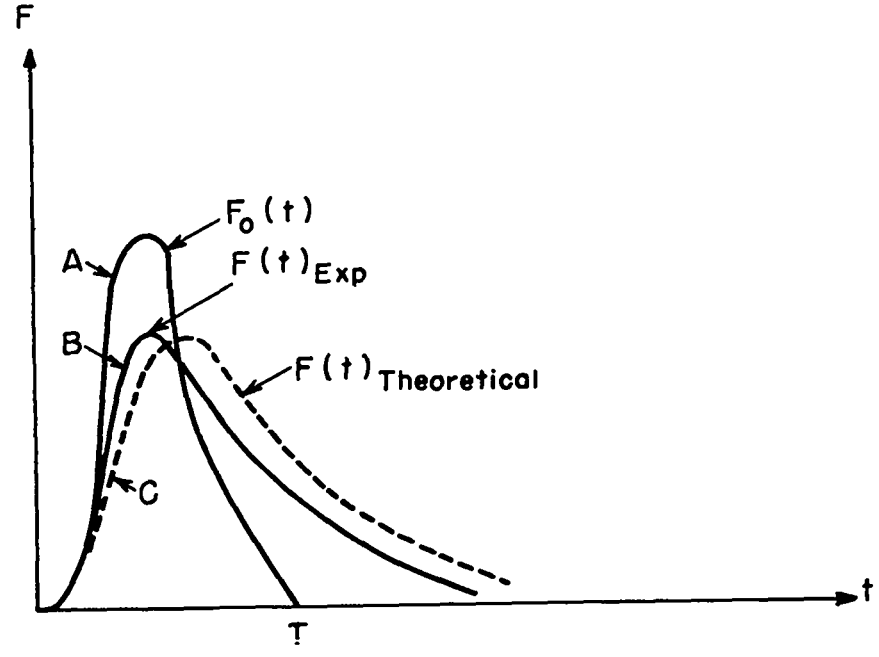

Figure 23. Influence of higher modes of neutron distribution upon fission response

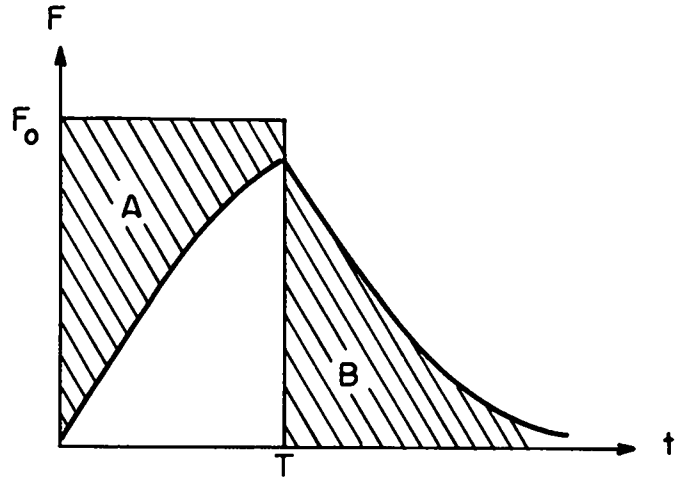

Figure 24. A or B represents delayed fissions if source pulse is rectangular.

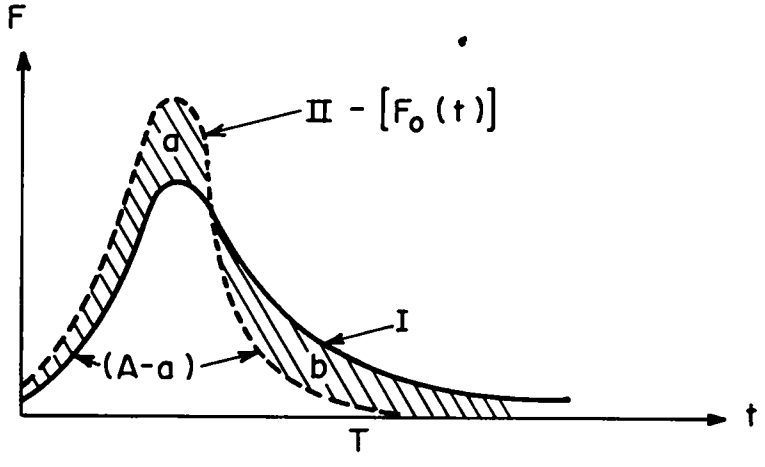

Figure 25. Delayed fissions (a or b) with actual source pulse. Curve I is observed U^{235} response, Curve II corresponds to zero decay constant.